JOC The Journal of Organic Chemistry

Open Access
This article is licensed under CC-BY-NC-ND 4.0

pubs.acs.org/joc Article

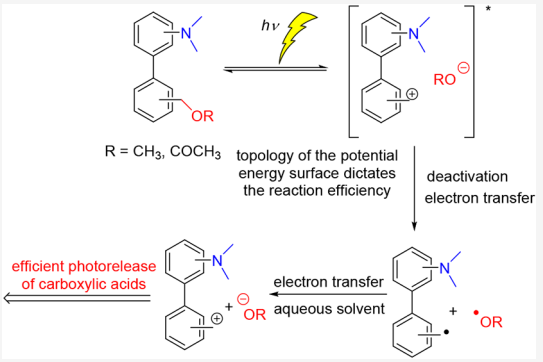
Heterolysis vs Homolysis and *ortho-meta*-Effects in the Photohydrolysis of Biphenylamine Photocages

Vilma Lovrinčević, Ivan Ljubić,* Igor Sviben, Mélyne Baudin-Marie, Lidija Uzelac, Marijeta Kralj, Irena Škorić, Dragana Vuk, and Nikola Basarić*

Cite This: J. Org. Chem. 2026, 91, 5947−5968 Read Online

ACCESS | Metrics & More | Article Recommendations | Supporting Information

ABSTRACT: Methyl ethers and acetyl esters of *N,N*-dimethylamino-hydroxymethylbiphenyls were synthesized with varying positions of the amino activating group and the methoxy or acetyl leaving group. Their photochemical reactivity was studied through photohydrolysis reactions to evaluate their potential as photocleavable protecting groups (PPGs) for the release of alcohols and carboxylic acids, respectively. The compounds were designed to investigate the *ortho-meta*-effects in biphenyl photochemistry. Photoreactivity was examined via irradiations in aqueous media, followed by isolation of photoproducts. The quantum yields of photoelimination (Φ_R) showed correlation with the *ortho-meta*-effects when both functional groups were located on the same aromatic ring, but not when distributed across different rings. To rationalize differences, potential energy surfaces for the CH_2−O bond cleavage were analyzed. Mechanistic insights were obtained using computational studies, fluorescence spectroscopy, and laser flash photolysis. The reaction proceeds via a heterolytic cleavage in the excited state, followed by the formation of benzyl radicals (τ = 25−50 μs) upon relaxation to the ground state. These radicals either recombine to form oligomers or undergo further electron transfer in aqueous solution, producing carbocations and acetate. The synthetic applicability was demonstrated through benzoyl and palmitoyl esters, which underwent photochemical cleavage with yields exceeding 70%.



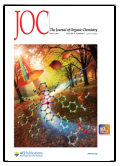
INTRODUCTION

The term "photocage" is used for a biologically active compound covalently linked to a chromophore and made temporarily inactive, which can be released in a photochemical reaction whereupon its activity is restored.[1] A closely related term more generally used in organic chemistry is photocleavable protective group (PPG).[2,3] Over the last few decades, scientists have developed a large number of PPGs based on different chromophores. They are cleaved off from substrates in photochemical reactions taking place via different mechanisms, which have been reviewed on several occasions.[4−9] For synthetic applications in particular, different chromophores were developed that enable selective and wavelength-dependent deprotection (so-called chromatic orthogonality).[10,11] Furthermore, significant progress has been made by developing PPGs that are based on chromophores absorbing visible light, thereby increasing their applicability in biology.[12]

The most commonly used photocages are *o*-nitrobenzyl,[13,14] coumarin-4-ylmethyl,[15−17] and *p*-hydroxyphenacyl derivatives.[18−23] Furthermore, decaging has been accomplished by benzophenone[24] or xanthone chromophores,[25] whereas the elimination of alcohols has been reported through the use of 2,5-dimethylphenacyl photocages.[26] Moreover, quinoline photocages[27,28] were developed and their applicability to release carboxylic acid under two-photon excitation has been demonstrated. Further elegant examples include fluorene[29] and indene photocages[30] that react efficiently owing to the antiaromatic character of 6π systems in the excited states.[31]

One large group of PPGs[32] release substrates in the photoelimination reactions that are based on the *meta*-effect in photochemistry.[33] Wang and Ding developed *m*-hydroxymethylaniline photocages for alcohols.[34] In the following reports Wang and Ding[35,36] extended the scope to *o*-hydroxymethylaniline photocages for alcohols and carboxylic acids. The photoreactivity of these *o*-aniline derivatives can be modified to release acids or alcohols by introducing a methyl group in the reactive center.[37] The decaging process was also demonstrated for amine derivatives.[38,39] However, the major obstacle in the use of aniline photocages is the fact that they absorb light at λ < 350 nm, which is mostly incompatible with

Received: January 29, 2026
Revised: March 25, 2026
Accepted: April 2, 2026
Published: April 17, 2026

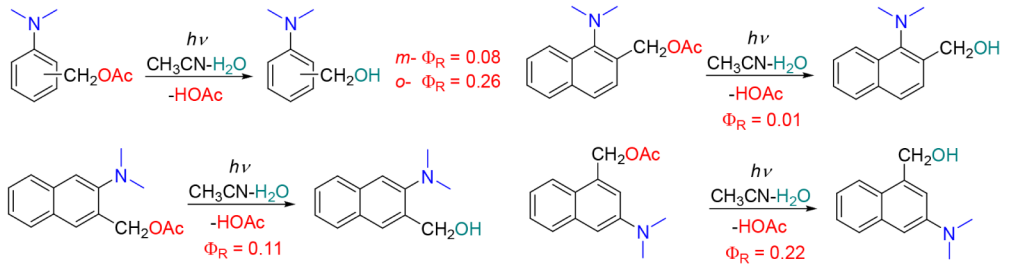


ACS Publications
© 2026 The Authors. Published by American Chemical Society

https://doi.org/10.1021/acs.joc.6c00228
J. Org. Chem. 2026, 91, 5947−5968

Downloaded from pubs.acs.org/joceah/article-pdf/91/17/5947/6205059/acs.joc.6c00228.pdf by RUDJER BOSKOVIC INST user on 05 October 2026

Scheme 1. Previously Investigated Aniline and Aminonaphthalene Photocages[34−36,41−43]



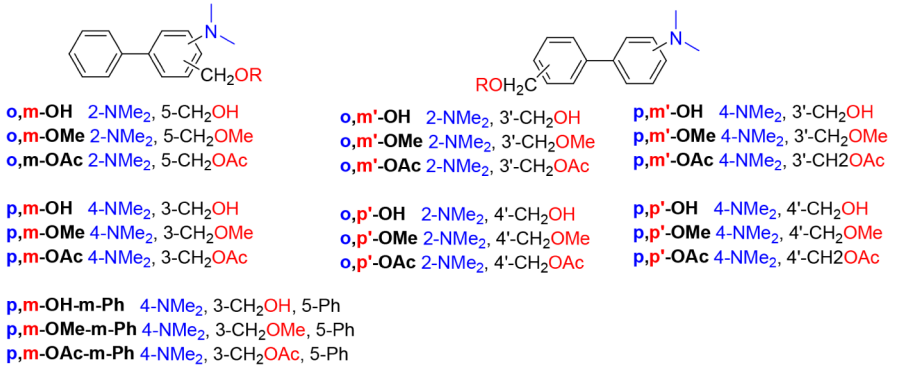
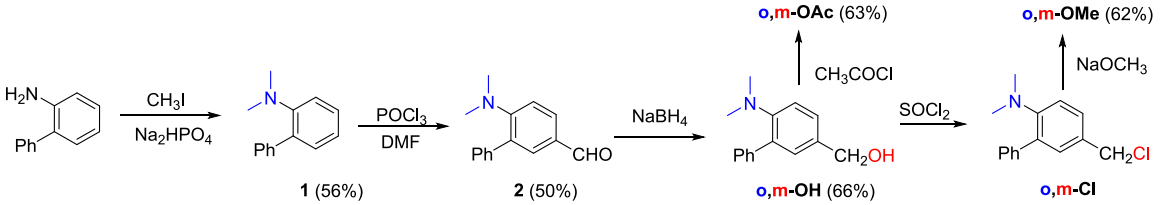


Figure 1. Investigated biphenylamine photocages (*o*-, *m*-, and *p*- refer to the position with respect to the biphenyl skeleton).

Scheme 2. Synthesis of Photocages o,m-OH



biological systems and many functional groups in organic molecules, so their use in biological systems was scarce.[40] Therefore, we developed *N,N*-dimethylaminonaphthalene photocages, which absorb in the near-visible region and can be used together with anilines for chromo-orthogonal deprotection.[41] The substitution pattern on the aminonaphthalene chromophores was investigated, indicating 2,3-[42] and 1,3-substituted aminonaphthalene derivatives[43] undergoing the most efficient photoelimination of acetic acid, Φ_R = 0.11 and Φ_R = 0.22, respectively (Scheme 1). The photoelimination mechanism was investigated by transient absorption spectroscopy (TAS) and computational methods. We found out that the mechanism involves homolytic cleavage to produce a radical pair that subsequently undergoes electron transfer to produce aminonaphthalene carbocation and the leaving group as acetate.[42,43] The competition between homolytic and heterolytic cleavage in the photochemical reactions has been investigated experimentally[44−47] and computationally across different systems.[48]

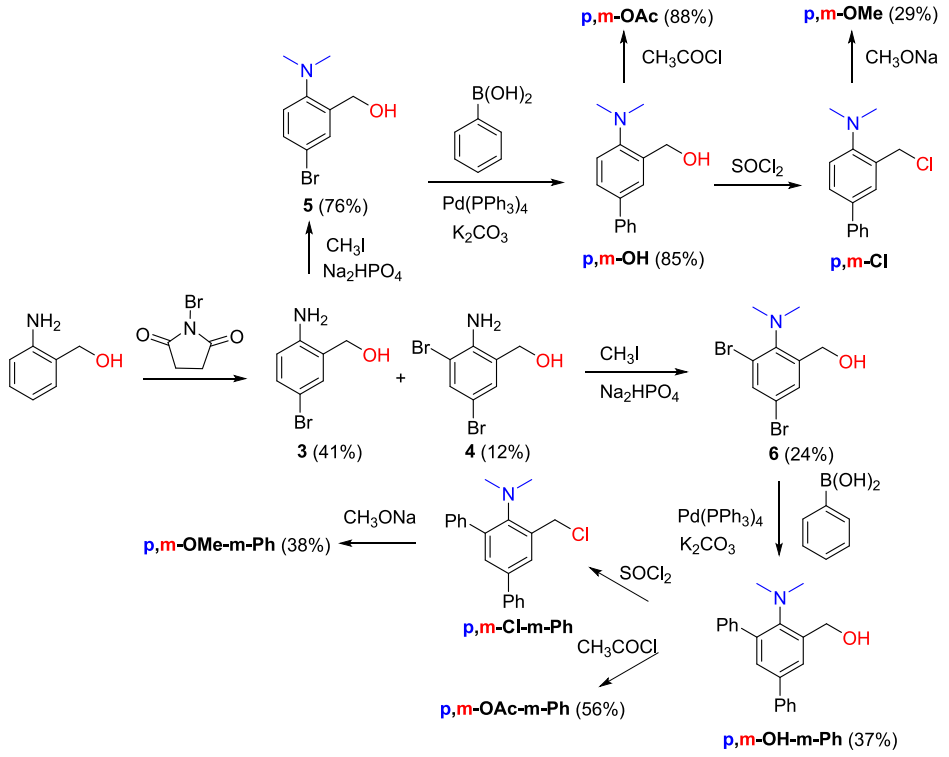
Herein, we report the synthesis and investigation of photochemical reactivity for a new line of biphenylamine photocages (Figure 1). The biphenylamine chromophore was systematically modified to investigate the effect of substitution on the photocleavage efficiency and its reaction mechanism. Furthermore, research directions will be oriented to developing push−pull aminobiphenyl chromophores undergoing decaging upon two-photon absorption. In these chromophores, the amino group is essential to activate the decaging process, as demonstrated by Wang for anilines,[7] as well as for other photocages such as *o*-nitrobenzyl derivatives.[49]

We prepared two series of photocages that have the amino-activating group and the methyl-releasing substituent in the same ring in the *ortho*- or the *para*-position, and a series of terphenyl derivatives with both groups in the middle ring. Furthermore, we investigated the extension of the *ortho-meta*-effect through conjugation in the biphenyl system. Thus, two series of photocages bear the amino-activating group in the *ortho*-position of the biphenyl chromophore but the releasing methyl group is in the adjacent ring in the *meta*- or the *para*-position. Analogously, two series have the amino group in the *para*-position, and the releasing substituent in the adjacent ring in the *meta*- or the *para*-position. The biphenyl derivatives with the amino group in the *meta*-position were not investigated experimentally since they can undergo photoredox reactions,[50] and some of them were investigated by Heckeel et al.[29] The reactivity was investigated by conducting preparative irradiations and isolation of photoproducts, whereas the mechanism of the reactions was investigated computationally and experimentally by fluorescence and TAS. The investigation indicated that the *ortho-meta* effect cannot be directly applied in the biphenyl systems, and to account for different photoreaction efficiencies, potential energy surfaces have to

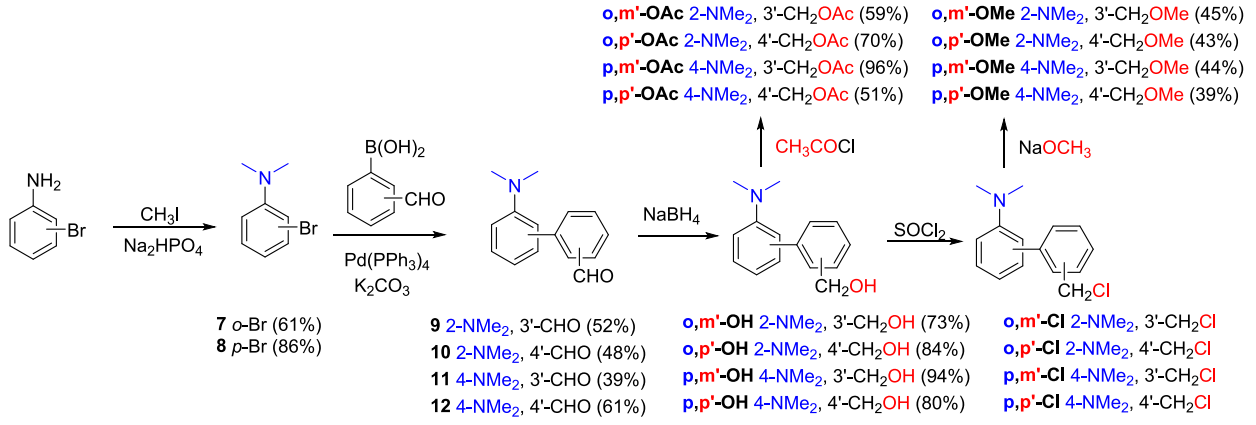
Downloaded from pubs.acs.org/joceah/article-pdf/91/17/5947/6205059/acs.joc.6c00228.pdf by RUDJER BOSKOVIC INST user on 05 October 2026

https://doi.org/10.1021/acs.joc.6c00228
J. Org. Chem. 2026, 91, 5947−5968

Scheme 3. Synthesis of Photocages p,m- and p,m-m-Ph



Scheme 4. Synthesis of Photocages with Substituents in Two Rings



be examined. Knowledge of all pathways and intermediates in the decaging is essential for the application of photocages in organic synthesis and biology since intermediates may interfere with different molecular structures of biologically important molecules.

RESULTS AND DISCUSSION

Synthesis

The synthesis of photocages reported herein is based on the preparation of alcohols, which were transformed into methyl ethers and acetyl esters as model compounds for the photorelease of alcohols or carboxylic acids, respectively. The synthesis of **o,m-OH** started from the commercially available 2-aminobiphenyl, which was methylated to **1** and the formyl group in the *para*-position to the amine was introduced in a Vilsmeier-Haack reaction (Scheme 2). The reduction by $NaBH_4$ afforded alcohol **o,m-OH**. The transformation of an alcohol to an acetyl derivative was accomplished in all examples by acetyl chloride. Methyl ethers were prepared by transforming alcohols to chlorides in the reaction with $SOCl_2$, followed by a nucleophilic substitution with NaOMe.

The synthesis of photocages **p,m-** and **p,m-m-Ph** started from commercially available 2-hydroxymethylaniline, which was brominated by NBS, affording mono- **3** and dibromoderivative **4**. They were then methylated on nitrogen to **5** and **6**, respectively (Scheme 3). The subsequent Suzuki coupling reaction yielded monoarylated alcohol **p,m-OH**, or terphenyl alcohol **p,m-OH-m-Ph**, respectively. The alcohols were transformed into ethers and esters, as described above.

The synthesis of photocages with substituents in two rings relies on a similar strategy as described for **p,m**-derivatives. The *ortho*- or *para*-bromoanilines were methylated to **7** and **8**, and arylated in the Suzuki reaction with *meta*- or *para*-formylphenylboronic acid and reduced to afford alcohols

https://doi.org/10.1021/acs.joc.6c00228
J. Org. Chem. 2026, 91, 5947−5968

Downloaded from pubs.acs.org/joceah/article-pdf/91/17/5947/6205059/acs.joc.6c00228.pdf by RUDJER BOSKOVIC INST user on 05 October 2026

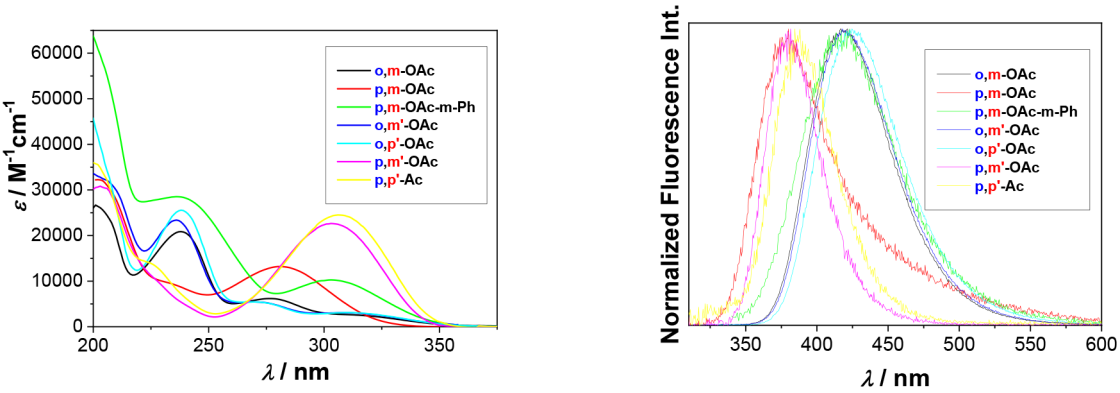


Figure 2. Absorption spectra of acetyl photocages in CH_3CN (left) and normalized fluorescence spectra in CH_3CN (λ_{ex} = 290 nm, right).

(Scheme 4). The alcohols were then transformed into the corresponding ethers and esters.

Photophysical Properties

Prior to the investigation of photochemical reactivity and the application of photocages, it is important to know their photophysical properties (for all spectra, see Figures S8−S47 in the SI). Therefore, absorption and fluorescence spectra of photocages were measured in CH_3CN (Figure 2 left). All absorption spectra exhibit maxima at λ = 275−350 nm, with distinctly different features depending on whether they are 2- or 4-aminobiphenyl derivatives. Thus, 2-amino derivatives (**o,m-**, **o,m'-**, and **o,p'-**) exhibit an absorption band with a maximum at λ = 270−280 nm, and a shoulder at ≈ 310 nm stretching to 350−360 nm. On the other hand, 4-amino biphenyl derivatives have one low-energy absorption band at ≈280 nm for **p,m-**derivatives and at 300−305 nm for **p,m'-** and **p,p'-** that stretch to 350 nm. The absorption maximum for the terphenyl derivatives is also at 300−305 nm. The introduction of the third phenyl ring shifted the absorption maximum bathochromically ≈ 20 nm (comparison of **p,m-** and **p,m-m-Ph**). The emission spectra in CH_3CN cluster with similar values for the maximum: 375−385 nm for 2-aminobiphenyls, or 420−425 nm for 4-aminobiphenyl and the terphenyl derivatives (Figure 2 right). Thus, 4-amino-biphenyls exhibit larger Stokes shifts (9000−11000 cm^{-1}) compared to 2-aminobiphenyls (5000−6000 cm^{-1}). However, none of the compounds exhibited dual emission that would be characteristic for the formation of the locally excited and charge transfer state. An increase in solvent polarity generally induced larger Stokes shifts (see Figure S48 in the SI) and higher quantum yields of fluorescence (Φ_F, Table 1, and S2 in the SI). The addition of H_2O to the CH_3CN solution only slightly shifts the emission maxima bathochromically.

The Φ_F values were measured using quinine sulfate in aqueous 0.05 M H_2SO_4 (Φ = 0.546),[51] whereas singlet excited state lifetimes were measured by time-correlated single photon counting (TC-SPC, Table 1). Higher values of Φ_F were generally measured for alcohols and methyl ethers than for esters, which is inversely correlated with the photochemical reactivity of acetyl derivatives (vide supra). Furthermore, 2-aminobiphenyl derivatives show lower Φ_F values in aqueous solution than in CH_3CN, which is also inversely correlated to higher photochemical reactivity in aqueous media. On the contrary, 4-aminobiphenyl acetyl derivatives show higher Φ_F values in aqueous solution, which is a general trend not connected to their photoreactivity in aqueous solution. Except for biphenyls **o,m-** that exhibit single exponential fluorescence decay, the decay of other compounds was fit to a sum of two or three exponents (for all decays, see Figures S49−S69 in the SI). The biexponential decay for arylamine derivatives has been reported and associated with the excited L_a and L_b states.[50,52]

In summary, fluorescence measurements indicated that molecules exhibit larger dipole moments in the singlet excited state compared to the S_0, but the formation of CT states has not been observed. A larger increase in dipole moment was observed for 4-aminobiphenyl derivatives than for 2-amino-biphenyls. The smallest values of Φ_F were observed for acetyl derivatives, which are the most photoreactive.

Photochemical Reactivity

The irradiation experiments of methyl ether and acetyl ester photocages were conducted in CH_3CN, or CH_3CN-H_2O (2:1) using lamps with a maximum output at ≈ 300 nm. The conversions and the isolated yields of photoproducts are compiled in Table 2. Formation of the corresponding alcohols was an indication that photohydrolysis and the elimination of CH_3OH or AcOH take place. Upon irradiation in CH_3CN, all compounds underwent decomposition without isolable photo-products. On the contrary, irradiation in the aqueous solvent gives rise to the photohydrolysis and the formation of the anticipated alcohols as main photoproducts (Scheme 5). The exception was the irradiation of **p,m-OMe-m-Ph** whereupon the hydrolysis did not take place, but the elimination of the methyl group from the nitrogen occurred, yielding **p,m-NHMe-m-Ph** (Table 2 and Figure 3). Similar demethylation was reported in the photochemistry of 2-substituted-1-naphthylamine ethers.[41] The photohydrolysis of esters was more efficient than the photohydrolysis of ethers, in accordance with OAc^- as a better leaving group than OMe^-. Furthermore, upon irradiation of **p,m'-OMe** and **p,m'-OAc**, in addition to alcohol **p,m'-OH**, the acetyl derivative **p,m'-NHAc** was isolated. Such an amide is the typical product of carbocation, probably formed in the photolysis, with acetonitrile. The irradiation of **p,p'-OMe** and **p,p'-OAc** also yielded the photooxidation product carbaldehyde **12**, although the irradiations were conducted in N_2-purged solutions.

For the reactions which were more efficient based on preparative irradiations (Table 2), quantum yields for the photohydrolysis (Φ_R, Table 3) were measured using a KI/KIO_3 actinometer (Φ_R = 0.74).[51] The photoelimination of alcohols is significantly less efficient than the elimination of carboxylic acids, with the highest value of Φ_R for the elimination of CH_3OH measured for **p,m'-OMe**. Furthermore,

Downloaded from pubs.acs.org/joceah/article-pdf/91/17/5947/6205059/acs.joc.6c00228.pdf by RUDJER BOSKOVIC INST user on 05 October 2026

https://doi.org/10.1021/acs.joc.6c00228
J. Org. Chem. 2026, 91, 5947−5968

Table 1. Photophysical Properties of Photocages

Compound	Φ_F (CH_3CN)[a]	τ(CH_3CN)/ns[b]	Φ_F(CH_3CN-H_2O)[c]	τ(CH_3CN–H_2O)/ns
o,m-OH	0.28 ± 0.02	4.87 ± 0.01 (1.0)		
o,m-OMe	0.29 ± 0.02	4.67 ± 0.07 (1.0)		
o,m-OAc	0.26 ± 0.02	4.56 ± 0.07 (1.0)		
p,m-OH	0.081 ± 0.035	0.03 ± 0.02 (0.09)	0.053 ± 0.001	0.03 ± 0.02 (0.09)
		2.21 ± 0.03 (0.82)		2.27 ± 0.05 (0.82)
		5.0 ± 0.6 (0.09)		4.6 ± 0.8 (0.09)
p,m-OMe	0.079 ± 0.002	0.05 ± 0.02 (0.08)	0.069 ± 0.004	0.04 ± 0.02 (0.09)
		2.10 ± 0.07 (0.70)		2.41 ± 0.05 (0.84)
		3.6 ± 0.3 (0.22)		5 ± 1 (0.07)
p,m-OAc	0.03 ± 0.01	0.05 ± 0.02 (0.15)	0.07 ± 0.04	0.05 ± 0.02 (0.10)
		2.25 ± 0.07 (0.61)		2.17 ± 0.11 (0.63)
		4.44 ± 0.30 (0.24)		3.40 ± 0.34 (0.27)
p,m-OH-m-Ph	0.046 ± 0.004	0.08 ± 0.06 (0.04)	0.066 ± 0.008	0.39 ± 0.08 (0.02)
		2.27 ± 0.004 (0.96)		3.324 ± 0.007(0.98)
p,m-OMe-m-Ph	0.052 ± 0.005	1.3 ± 0.2 (0.08)	0.069 ± 0.003	1.61 ± 0.1 (0.17)
		2.58 ± 0.03 (0.92)		3.48 ± 0.04 (0.83)
p,m-OAc-m-Ph	0.014 ± 0.001	0.466 ± 0.005 (0.73)	0.009 ± 0.003	0.16 ± 0.01 (0.30)
		3.50 ± 0.03 (0.27)		2.7 ± 0.2 (0.49)
				5.3 ± 0.8 (0.21)
o,m'-OH	0.14 ± 0.05	0.06 ± 0.04 (0.04)	0.16 ± 0.05	0.09 ± 0.06 (0.02)
		4.31 ± 0.01 (0.96)		7.28 ± 0.01 (0.98)
o,m'-OMe	0.36 ± 0.01	0.03 ± 0.05 (0.02)	0.30 ± 0.01	0.12 ± 0.05 (0.02)
		5.31 ± 0.01 (0.98)		6.39 ± 0.01 (0.98)
o,m'-OAc	0.40 ± 0.01	0.3 ± 0.06 (0.03)	0.34 ± 0.01	0.04 ± 0.02 (0.04)
		6.04 ± 0.01 (0.97)		3.5 ± 0.2 (0.39)
				6.2 ± 0.2 (0.57)
o,p'-OH	0.26 ± 0.05	0.09 ± 0.04 (0.03)	0.32 ± 0.07	0.02 ± 0.01(0.02)
		5.26 ± 0.01 (0.97)		7.46 ± 0.01 (0.98)
o,p'-OMe	0.30 ± 0.01	1.4 ± 0.2 (0.04)	0.49 ± 0.02	3.0 ± 0.4 (0.04)
		4.34 ± 0.02 (0.96)		8.04 ± 0.04(0.96)
o,p'-OAc	0.144 ± 0.003	1.7 ± 0.1 (0.71)	0.04 ± 0.02	0.232 ± 0.005 (0.36)
		2.4 ± 0.4 (0.29)		6.75 ± 0.03 (0.64)
p,m'-OH	0.73 ± 0.02	0.03 ± 0.02 (0.07)	0.60 ± 0.04	0.42 ± 0.06 (0.07)
		2.69 ± 0.02 (0.91)		2.37 ± 0.01 (0.93)
		9 ± 3 (0.02)		
p,m'-OMe	0.93 ± 0.03	0.6 ± 0.1 (0.04)	0.54 ± 0.02	0.09 ± 0.03 (0.08)
		2.67 ± 0.01 (0.96)		2.03 ± 0.01 (0.92)
p,m'-OAc	0.025 ± 0.005	0.047 ± 0.007 (0.39)	0.12 ± 0.01	0.02 ± 0.01 (0.08)
		2.53 ± 0.04 (0.57)		2.48 ± 0.03 (0.44)
		14 ± 7 (0.04)		10.9 ± 0.1 (0.48)
p,p'-OH	0.84 ± 0.14	0.03 ± 0.02 (0.08)	0.72 ± 0.08	0.08 ± 0.04 (0.07)
		2.18 ± 0.07 (0.84)		2.02 ± 0.02 (0.89)
		4 ± 1 (0.08)		8 ± 1 (0.04)
p,p'-OMe	0.83 ± 0.08	0.94 ± 0.2 (0.09)	0.72 ± 0.07	0.07 ± 0.03 (0.09)
		2.07 ± 0.014 (0.91)		1.87 ± 0.02 (0.88)
				5.93 ± 1 (0.03)
p,p'-OAc	0.020 ± 0.004	0.013 ± 0.003 (0.72)	0.25 ± 0.02	0.04 ± 0.04 (0.11)
		2.8 ± 0.08 (0.23)		2.09 ± 0.02 (0.72)
		45.10 ± 11 (0.05)		10.8 ± 0.3 (0.17)

[a]Quantum yield of fluorescence was measured using quinine sulfate in aqueous 0.05 M H_2SO_4 (Φ = 0.546).[51] One fluorescence measurement was performed by exciting the sample at three different wavelengths, and the average value was calculated. The quoted errors correspond to the maximal standard deviation. [b]Decay times from the singlet excited state (τ) were measured by TC-SPC. The samples were excited at 340 nm. One decay was collected, and the quoted errors were obtained from fitting to a sum of exponentials. Numbers in parentheses correspond to the weighted contribution of decay components. [c]The measurements were performed in CH_3CN-H_2O (4:1) in the presence of sodium phosphate buffer 50 mM, pH = 7.0.

the amino group activates the elimination of the acetyl in biphenyl molecules from the same ring, but also from the adjacent ring. The elimination from biphenyls **o,m-** and **p,m-**, where both groups are in the same ring, follows the typical pattern anticipated from the *ortho-meta*-effect in photochemistry;[33] that is, it activates the *ortho*-position (these results) and the *meta*-position.[29] The quantum yield for the release of the acetyl group from the *ortho*-substituted aniline (Φ_R = 0.26)[36] and **p,m-OAc** (Φ_R = 0.22) is similar. The unprecedented finding is that the introduction of an additional

https://doi.org/10.1021/acs.joc.6c00228
J. Org. Chem. 2026, 91, 5947−5968

Downloaded from pubs.acs.org/joceah/article-pdf/91/17/5947/6205059/acs.joc.6c00228.pdf by RUDJER BOSKOVIC INST user on 05 October 2026

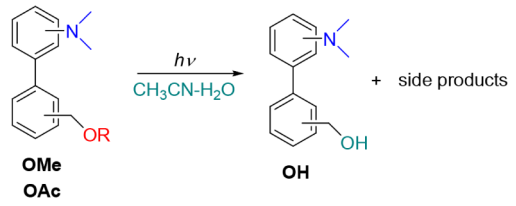
Table 2. Irradiation Conditions, Conversion to Products and Isolated Yields after the Irradiation of Photocages

Comp.	Irradiation conditions[a]	Conversion (%)[b]	Products and yields (%)[c]
o,m-OMe	CH_3CN, 4 h	15	Decomposition
o,m-OMe	CH_3CN-H_2O (2:1), 4 h	14	**o,m-OH** (14)
o,m-OAc	CH_3CN, 4 h	30	Decomposition
o,m-OAc	CH_3CN-H_2O (2:1), 4 h	33	**o,m-OH** (32)
p,m-OMe	CH_3CN, 4 h	66	Decomposition
p,m-OMe	CH_3CN-H_2O (2:1), 4 h	30	**p,m-OH** (24)
p,m-OAc	CH_3CN, 4 h	65	Decomposition
p,m-OAc	CH_3CN-H_2O (2:1), 1 h	80	**p,m-OH** (78)
p,m-OMe-m-Ph	CH_3CN, 4 h	55	Decomposition
p,m-OMe-m-Ph	CH_3CN-H_2O(2:1), 4 h	30	**p,m-NHMe-m-Ph** (20)
p,m-OAc-m-Ph	CH_3CN, 4 h	43	Decomposition
p,m-OAc-m-Ph	CH_3CN-H_2O (2:1), 4 h	42	**p,m-OH-m-Ph** (39)
o,m'-OMe	CH_3CN, 4 h	36	Decomposition
o,m'-OMe	CH_3CN-H_2O (2:1), 4 h	10	**o,m'-OH** (8)
o,m'-OAc	CH_3CN, 4 h	42	Decomposition
o,m'-OAc	CH_3CN-H_2O (2:1), 1.5 h	77	**o,m'-OH** (72)
o,p'-OMe	CH_3CN, 4 h	24	Decomposition
o,p'-OMe	CH_3CN-H_2O (2:1), 4 h	17	**o,p'-OH** (11)
o,p'-OAc	CH_3CN, 4 h	75	Decomposition
o,p'-OAc	CH_3CN-H_2O (2:1), 1 h[d]	86	**o,p'-OH** (85)
o,p'-OAc	CH_3CN-H_2O (2:1), 1 h[e]	90	**o,p'-OH** (85)
o,p'-OAc	CH_3CN-H_2O (2:1), 0.5 h	87	**o,p'-OH** (82)
p,m'-OMe	CH_3CN, 4 h	64	Decomposition
p,m'-OMe	CH_3CN-H_2O (2:1), 2 h	83	**p,m'-OH** (52) + **p,m'-NHAc** (29)
p,m'-OAc	CH_3CN, 4 h	82	Decomposition
p,m'-OAc	CH_3CN-H_2O (2:1), 1 h	95	**p,m'-OH** (43) + **p,m'-NHAc** (52)
p,p'-OMe	CH_3CN, 4 h	66	Decomposition
p,p'-OMe	CH_3CN-H_2O (2:1), 4 h	55	**p,p'-OH** (30) + **12** (22)
p,p'-OAc	CH_3CN, 4 h	75	Decomposition
p,p'-OAc	CH_3CN-H_2O (2:1), 1 h	60	**p,p'-OH** (27) + **12** (18)

[a]The irradiations were conducted in N_2-purged solutions (c = 0.001 M) in a Luzchem photoreactor equipped with 8 lamps with a maximum output at ≈ 300 nm (one lamp ≈ 8 W). The irradiated solution was placed in quartz test tubes positioned in the middle of the reactor, equally separated (15 cm) from 4 lamps on each side. [b]The conversion was determined by HPLC. [c]Isolated yields and some structures of side-products are shown in Figure 3. [d]Irradiation was conducted in N_2-purged solution (c = 0.003 M). [e]Irradiation was conducted in O_2-purged solution (c = 0.003 M).

phenyl ring in **p,m-OAc-m-Ph** decreased the photoreaction efficiency by about four times, based on the results from preparative irradiations (Table 2). However, the *ortho-meta*-effect for the elimination from biphenyl derivatives with the amino group in one ring and the leaving acetyl group in the other is not straightforward. Generally, the amino group in the

Scheme 5. Photohydrolysis from OMe and OAc Photocages; for Side Products see Figure 3 and Table 2



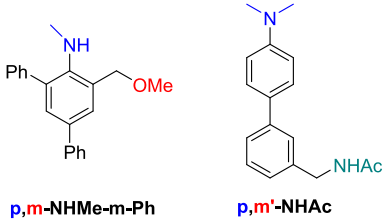


Figure 3. Side products formed upon irradiation of **p,m-OMe-m-Ph**, **p,m'-OMe**, and **p,m'-OAc**.

Table 3. Quantum Yields for the Photohydrolysis (Φ_R)[a]

Comp.	Φ_R
p,m-OAc	0.22 ± 0.01
o,m'-OAc	0.13 ± 0.01
o,p'-OAc	0.37 ± 0.01
p,m'-OAc	0.16 ± 0.01
p,m'-OMe	0.003 ± 0.002

[a]Φ_R values were determined using a KI/KIO_3 actinometer (Φ_R = 0.74)[S1] upon excitation by monochromatic irradiation at 254 nm.

ortho-position of the biphenyl skeleton had a stronger activating effect for the acetyl elimination from the adjacent ring than the amino group in the *para*-position. However, the elimination from the *meta*-benzylic position in **o,m'-OAc** is less efficient than the elimination from the *para*- in **o,p'-OAc**, which is not in accord with the *ortho-meta*-effect. On the contrary, the amino group in the *para*-position in **p,m'-OAc** activates more the leaving group in the *meta*-position in the adjacent ring more than in the *para*-position (in **p,p'-OAc**), which is in accord with the *ortho-meta*-effect.

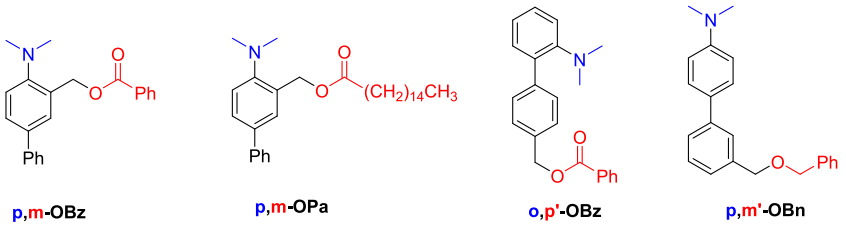
The application of biphenylamine photocages in organic synthesis was demonstrated for the elimination of benzoic acid and palmitic acid from the most efficient releasing PPGs based on **p,m-OAc**, **o,p'-OAc** and **p,m'-OAc**. The corresponding esters benzoates (**p,m-OBz**, **o,p'-OBz** and **p,m'-OBz**) and palmitates (**p,m-OPa**, **o,p'-OPa** and **p,m'-OPa**) were prepared in the reactions of chlorides **p,m-Cl**, **o,p'-Cl** and **p,m'-Cl** with carboxylates, benzoate, or palmitate, respectively (see the experimental). The photocages were irradiated in CH_3CN-H_2O (2:1) at ≈ 300 nm, whereupon the alcohols were regenerated, and the carboxylic acids were isolated in good to excellent yields (Table 4). A preparative irradiation was also conducted for photocage **p,m'-OBn** to release the benzylic alcohol, which was isolated in moderate yield after a very long irradiation. Thus, the biphenylamine photocages are excellent in releasing both aliphatic and aromatic carboxylic acids, but not alcohols.

Since laser flash photolysis (LFP) measurements indicated the formation of benzyl radicals in the photolyzes (vide infra), the irradiations of **o,p'-OAc** and **p,m'-OAc** were conducted

Downloaded from pubs.acs.org/joceah/article-pdf/91/17/5947/6205059/acs.joc.6c00228.pdf by RUDJER BOSKOVIC INST user on 05 October 2026

https://doi.org/10.1021/acs.joc.6c00228
J. Org. Chem. 2026, 91, 5947−5968

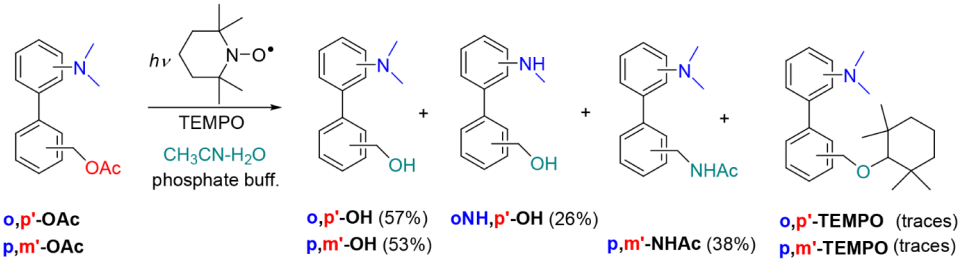
Table 4. Yields of Benzoic Acid, Palmitic Acid and Benzylic Alcohol in the Preparative Irradiations of Photocages



Comp.	Irradiation conditions[a]	Conversion (%)[b]	Photoproducts and isolated yields (%)[c]
p,m-OBz	$CH_3CN–H_2O$ (2:1), 5 h	76	**p,m-OH** (55) + benzoic acid (74)
p,m-OPa	$CH_3CN–H_2O$ (2:1), 6 h	82	**p,m-OH** (54) + palmitic acid (81)
o,p'-OBz	$CH_3CN–H_2O$ (2:1),4.5 h	89	**o,p'-OH** (61) + benzoic acid (79)
o,p'-OPa	$CH_3CN–H_2O$ (2:1), 5 h	93	**o,p'-OH** (75) + palmitic acid (90)
p,m'-OBz	$CH_3CN–H_2O$ (2:1), 9 h	82	**p,m'-OH** (13) + **p,m'-NHAc** (69) + benzoic acid (79)
p,m'-OPa	$CH_3CN–H_2O$ (2:1), 14 h	87	**p,m'-OH** (7) + **p,m'-NHAc** (80) + palmitic acid (84)
p,m'-OBn	$CH_3CN–H_2O$ (2:1), 40 h	78	**p,m'-OH** (23) + **p,m'-NHAc** (33) + benzylic alcohol (43)

[a]The irradiations were conducted in N_2-purged solutions in a Rayonet reactor equipped with 12 lamps with a maximum output at ≈ 300 nm (one lamp ≈ 8 W). The irradiated solution was placed in a quartz test tube positioned in the middle of the reactor, equally separated (10 cm) from the lamps. [b]The conversion was determined by HPLC. [c]Isolated yields.

Scheme 6. Irradiation of Photocages in the Presence of TEMPO



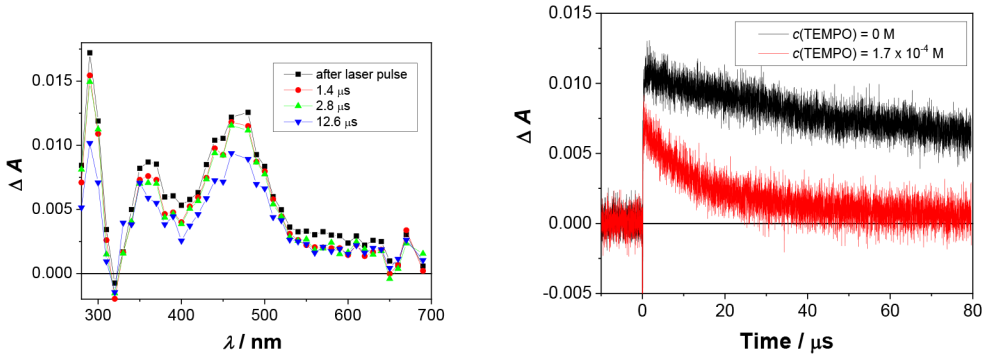


Figure 4. Transient absorption spectra of **o,p'-OAc** in $CH_3CN–H_2O$ (1:1) in the presence of sodium phosphate buffer (c = 0.05 M, pH = 7.0) in O_2-purged solution (left) and decay of transient absorption at 450 nm for the nonpurged aqueous buffered solution of **o,p'-OAc** without and in the presence of TEMPO (right).

also in the aqueous buffered solution in the presence of 2,2,6,6-tetramethylpiperidine-1-oxyl (TEMPO), which is the well-known radical scavenger.[53] However, the anticipated radical trapping products were detected only as traces by HPLC-MS (Scheme 6). Instead, the photolyzes gave rise to the corresponding alcohols as the main products, *N*-demethylation product **oNH,p'-OH**, and acetyl product **p,m'-NHAc** (see Figures S1–S7 in the SI). Detection of only traces of the TEMPO adducts may be rationalized by the photochemical reactivity of these adducts, presumably more efficient than the reactivity of acetyl precursors. Furthermore, the formation of *N*-dealkylation in the presence of TEMPO has been documented in the photochemistry of a 7-diethylaminocoumarin derivative.[17] It was rationalized by an H-abstraction reaction from the *N*-alkyl group by TEMPO. Moreover, *N*-dealkylation from tertiary amines by TEMPO has been documented in thermal[54] and electrochemical processes.[55]

Transient Absorption Spectroscopy

The investigation of the photochemical reaction mechanism for the elimination of acetate from *ortho*-substituted anilines revealed heterolytic cleavage giving *ortho*-aminobenzyl cation and acetate as a leaving group.[36] On the contrary, photoelimination of acetate from different aminonaphthalenes takes place homolytically, giving a radical pair that subsequently in an electron transfer yields a carbocation and acetate.[42,43] Thus,

https://doi.org/10.1021/acs.joc.6c00228
J. Org. Chem. 2026, 91, 5947–5968

Downloaded from pubs.acs.org/joceah/article-pdf/91/17/5947/6205059/acs.joc.6c00228.pdf by RUDJER BOSKOVIC INST user on 05 October 2026

photohydrolysis from aminobiphenyl derivatives can, in principle, proceed either homolytically or heterolytically. To investigate the photochemical reaction mechanism and detect plausible reactive intermediates in the photohydrolysis, LFP experiments were conducted for **p,m-OAc**, **o,m'-OAc**, **o,p'-OAc** and **p,m'-OAc** that show the highest values of Φ_R for the photoelimination of acetate. The TAS were measured in CH_3CN and CH_3CN-H_2O (1:1 in the presence of phosphate buffer, pH 7.0, 50 mM), where differences were anticipated, as photocages delivered hydrolysis product in aqueous solution only. Moreover, the measurements were conducted in N_2- and O_2-purged solutions, where O_2 was anticipated to quench triplet excited states and radicals, but not carbocations (for all data, see Figures S70−S87 in the SI).

In the N_2-purged CH_3CN solution of **o,p'-OAc** transients were detected absorbing over the whole visible region with a maximum at 430 nm (after the laser pulse), which evolved into spectra with two maxima at ≈350 nm and ≈ 470 nm (Figure S71). The decay of transient absorption was fit to a sum of three exponents with rate constants corresponding to decay times of 920 ± 40 ns, 5 ± 2 μs, and 60 ± 30 μs, and it was not quenched by O_2. In the buffered aqueous solution of **o,p'-OAc** the spectra (Figure 4) are similar to those in CH_3CN, but the decay was slower. Thus, in the O_2-purged aqueous solution, the decay was fit to a sum of three exponents corresponding to lifetimes of 600 ± 50 ns (faster decay under O_2), 38 ± 2 μs, and 400 ± 30 μs.

Based on the comparison with the TAS for the *ortho*-aminobenzyl cation (λ_{max} = 400 nm, τ = 90 μs),[36] the main transient from **o,p'-OAc** with the lifetime of τ = 38 μs detected in the O_2-purged aqueous solution may correspond to a carbocation **o,p'-cat** (Figure 5). Therefore, we conducted

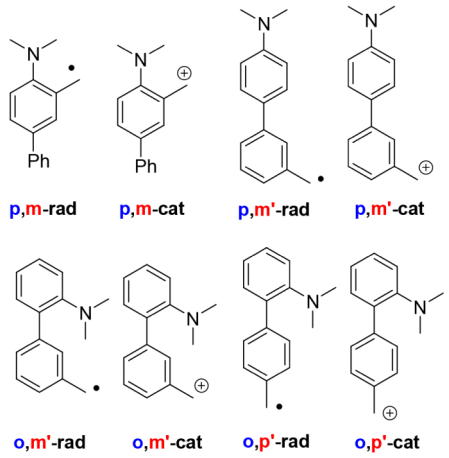


Figure 5. The anticipated and detected transients from **p,m-OAc**, **o,m'-OAc**, **o,p'-OAc**, and **p,m'-OAc**.

quenching experiments with sodium azide, the ubiquitous quencher that reacts with carbocations at a rate approaching the diffusion limit.[56] However, the azide does not quench the transients from **o,p'-OAc** with the lifetime of τ = 38 μs. In the presence of NaN_3, only the intensity of the transient absorption was lower, suggesting that it quenched the precursor to the transient with a lifetime of τ = 38 μs (Figure S73 in the SI). Furthermore, NaN_3 might have affected the long-lived transient, but its quenching could not be studied due to the very low intensity, which precluded the use of a nonpulsed lamp in the LFP measurement.

To assign the transients, the quenching was also conducted with TEMPO. In neat CH_3CN, the transient with the maximum at 470 nm was quenched (Figure 4 right) with the rate constant k_q = 9.3 ± 0.7 × 10^8 $M^{-1}s^{-1}$ (Figures S74 and S75 in the SI) and a similar value was determined for the quenching in aqueous buffered solution, k_q = 3.0 ± 0.5 × 10^8 $M^{-1}s^{-1}$. Thus, the main transient with a lifetime of ≈ 40 μs detected both in CH_3CN and in the aqueous buffered solution corresponds to the benzylic free radical **o,p'-rad**. It is interesting to note that this radical has the same decay constant in the N_2- and O_2-purged solution. This may be rationalized by its structure, with an important resonance contribution and spin density localized on the nitrogen, decreasing its ubiquitous radical reactivity, as seen with aminonaphthyl radicals.[42,43] We considered also the possibility that the detected transient corresponds to the carbocation in the triplet ground state. Carbocations that have triplet ground state have been documented in the cases when they are stabilized by strong electron donating substituents.[17,46,47,57] However, computations revealed that the singlet cation **o,p'-cat** is lower in energy then the corresponding triplet by 10.1 kcal mol^{-1}. It should also be emphasized that, upon addition of TEMPO, the transient with the long lifetime of 400 ± 30 μs was not detected. Therefore, it was assigned to the carbocation **o,p'-cat** that is formed from the radical by electron transfer. In the presence of TEMPO, the cation was not formed.

TAS for **o,m'-OAc** look very similar to those of **o,p'-OAc** in both CH_3CN and aqueous buffered solution, since these are both 2-aminobiphenyl derivatives and exhibit similar reactivity (see Figures S76−S79 in the SI). Thus, LFP experiments for **o,m'-OAc** also enabled detection of the benzyl radical **o,m'-rad**, absorbing at λ ≈ 470 nm with a lifetime of τ ≈ 40−50 μs. It also decays by electron transfer, yielding benzylic carbocation **o,m'-cat** with longer lifetime.

The TAS for **p,m-OAc** and **p,m'-OAc**, which are 4-aminobiphenyl derivatives, look different from the above-described (see Figures S80−S87 in the SI). In the N_2-purged CH_3CN solution of **p,m'-OAc** transients were detected absorbing over the whole visible region with two maxima at ≈ 370 nm and ≈ 640 nm (Figure S81). The decay was fit to a sum of two exponents, with rate constants corresponding to decay times of 110 ± 10 ns (350 nm), and 18 ± 2 μs. By purging the solution with O_2 the spectra qualitatively looked the same, but the decay was fit to a sum of three exponents with rate constants corresponding to decay times of ≈15 ns (350 ns), 5.1 ± 0.3 μs (350 nm), and 25 ± 5 μs. Furthermore, in the buffered aqueous solution of **p,m'-OAc** the spectra are similar to those in CH_3CN (Figure S82), but the decay was slower. Thus, in the O_2-purged solution, the decay was fit to a sum of two exponents corresponding to lifetimes of 25 ± 2 μs and 240 ± 10 μs (650 nm). To assign the main transient with the lifetime of 25 μs, quenching with NaN_3 was conducted, but it was not quenched, indicating that it does not correspond to carbocation **p,m'-cat**.

TAS for **p,m-OAc** and **p,m'-OAc** look very similar, both with two maxima at ≈ 370 nm and ≈ 640 nm. In the O_2-purged CH_3CN solution of **p,m-OAc** (Figure S84) the decay was fit to a sum of three exponents with rate constants corresponding to decay times of ≈ 20 ns, 7 ± 2 μs, and 28 ± 8 μs. In contrast, in the buffered aqueous solution (Figure 6 left and Figure S85 in the SI) which was not purged, the decay was fit to a sum of three exponents corresponding to lifetimes ≈ 200 ns, 35 ± 5 μs, and 200 ± 30 μs. Upon addition of NaN_3

Downloaded from pubs.acs.org/joceah/article-pdf/91/17/5947/6205059/acs.joc.6c00228.pdf by RUDJER BOSKOVIC INST user on 05 October 2026

https://doi.org/10.1021/acs.joc.6c00228
J. Org. Chem. 2026, 91, 5947−5968

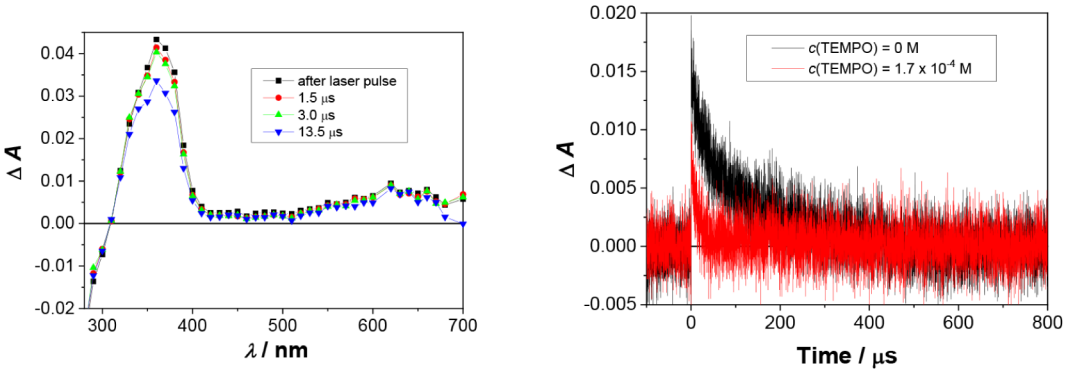


Figure 6. Transient absorption spectra of **p,m-OAc** in CH_3CN-H_2O (1:1) in the presence of sodium phosphate buffer (c = 0.05 M, pH = 7.0) in O_2-purged solution (left). Decay of transient absorption at 620 nm for the nonpurged aqueous buffered solution of **p,m-OAc** without and in the presence of TEMPO.

the main transient with a lifetime of 35 μs was not quenched, indicating that it is not the carbocation **p,m-cat**. However, it was quenched by TEMPO in CH_3CN and in the aqueous buffered solution (Figure 6 right and Figures S86 and S87 in the SI) with rate constants $k_q = 9 \pm 1 \times 10^8$ $M^{-1}s^{-1}$ and $k_q = 2.1 \pm 0.3 \times 10^8$ $M^{-1}s^{-1}$, respectively. Consequently, the transients from **p,m-OAc** and **p,m'-OAc** with a maximum of absorption at $\lambda \approx 650$ nm and lifetimes of 25 or 35 μs, were assigned to benzyl radicals **p,m-rad** and **p,m'-rad**. They also probably decay by electron transfer yielding longer-lived carbocations **p,m-cat** and **p,m'-cat** $\tau > 200$ μs.

In summary, LFP experiments allowed for the detection of benzylic radicals. The formation of carbocations from radicals was not directly proven, but it was inferred from the quenching with TEMPO, whereupon long-lived transients assigned to carbocations were not observed.

Computational Study

To unravel the mechanistic details of the photocleavage, a computational study was conducted (for computational details, see the Experimental section) for acetyl photocages shown in Figure 1, and for the compounds **m,m'-OAc** and **m,p'-OAc** (Figure S88 in the SI) which were not experimentally investigated in this study.

In all the **OAc** isomers, the S_1 state is dominated by the HOMO→LUMO transition; the corresponding CIS amplitudes are, in all cases, larger than 0.9. This applies equally to the Franck−Condon (FC) geometries and the optimized S_1 minima. The main features of the HOMO and LUMO remain similar in the FC geometries and the S_1 minima (Figures S89 and S90 in the SI). The computed absorption spectra require red-shifting by ca. 0.3 eV to bring them in good agreement with the measured spectra (Figure 1 and Table S3). The most conspicuous difference between the isomers is in the strongly varying intensity of the S_1 (HOMO→LUMO) transition found just above 300 nm. Specifically, the S_1 bands of **p,m'-OAc** and **p,p'-OAc** are very intense whereas those of the remaining isomers are weak, which is well reproduced by the computations (Table S3). The key difference is that **p,m'-OAc** and **p,p'-OAc** possess the *para*-amino group (4-NMe_2), which is the only position that topologically allows for ample delocalization of the electron density to the adjacent −CH_2OAc-substituted phenyl ring in the HOMO (Figure S89). Such delocalization dramatically enhances the oscillator strength of the HOMO→LUMO excitation. One should also note the trend in the charge translocation upon the HOMO→LUMO transition, which is most pronounced in **m,m'-OAc** and **m,p'-OAc**, followed by isomers **o,m'-OAc** and **o,p'-OAc**, and the smallest for isomers **p,m'-OAc** and **p,p'-OAc**. Such a finding is in agreement with the *ortho-meta*-effect.

The predicted ordering of the emission maxima for the five **OAc** isomers (Table S4 in the SI) correlates well with their ordering in the measured fluorescence spectra (Figure 2 right). The distances between the maxima are also reproduced reasonably well (Table S4). The computed values are best aligned with the measured ones upon applying a red shift of ca. 0.2 eV (note, however, that the absorption and emission spectra were recorded in CH_3CN, whereas the computations use the CPCM parameters for H_2O). The most conspicuous error pertains to the interchanged ordering of the **o,m'-OAc** and **o,p'-OAc** maxima. This, however, holds for the *syn*-conformer of **o,m'-OAc**, whereas the maximum of *anti*-**o,m'-OAc**, owing to the less staggered biphenyl rings, is indeed slightly blue-shifted relative to **o,p'-OAc**, agreeing better with the measured spectra. We still note that *syn*-**o,m'-OAc** is surprisingly predicted to be lower in energy than *anti*-**o,m'-OAc**. This is reminiscent of the *gauche*- (or similarly the *syn*-) effect, whereby the preferred conformers are curiously those in which strongly electronegative atoms reside on the same side and thus are mutually closer.[58,59] Considering that the fluorescence spectra suggest that the *anti*-conformation plays a role in the photophysics of **o,m'-OAc**, we analyzed the dissociation curves corresponding to both **o,m'-OAc** conformers (vide infra).

By performing relaxed energy scans along the H_2C−OAc distance on the S_1 surface, we produced potential energy curves for the photodissociating C−O bond in the **OAc** isomers (Figure 7). The dissociation curves for selected **OH** and **OMe** isomers are provided in the SI (Figure S91 in the SI). It can be noticed that common to all the dissociation curves is the potential maximum (loosely corresponding to the point of the C−O bond scission), followed by the descent, which can be further characterized according to its steepness. The barrier for the C−O bond scission in the S_1 state is estimated as the energy difference between the S_1 minimum and the maximum of the dissociation curve (Table 5).

On elongating the C−O distance from 1.4 to 2.8 Å, the gap between the S_0 and S_1 states gradually decreases from the initial >3 eV to ca. 1.5 eV. The two notable exceptions are **p,p'-OAc** and **p,m-OAc**. In the former case, the gap at the final point (d(C−O) = 2.8 Å) is considerably larger, around 2.3 eV. Conversely, in the latter case, the S_0/S_1 gap closes significantly

Downloaded from pubs.acs.org/joceah/article-pdf/91/17/5947/6205059/acs.joc.6c00228.pdf by RUDJER BOSKOVIC INST user on 05 October 2026

https://doi.org/10.1021/acs.joc.6c00228
J. Org. Chem. 2026, 91, 5947−5968

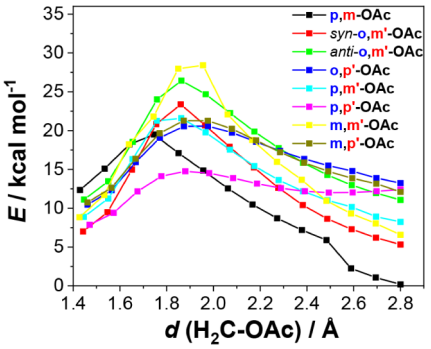


Figure 7. Dissociation curves for the H_2C-OAc bond of the **OAc** isomers computed at the TD-CAM-B3LYP-D4/def2-SVPD level. The CPCM parameters for the water solvent were used. The energy values were normalized with respect to the minimal computed energy for compound **p,m-OAc**, which arbitrarily has a value of 0 kcal mol^{-1}.

quicker than in the remaining **OAc** isomers, causing the S_0 and S_1 surfaces to intersect already at the 2.8 Å C−O distance.

Because the departing **OAc** group readily assumes the negative ionic (acetate) form, the dissociations on the S_1 surface are all heterolytic in nature, which is confirmed by analyzing the total charges on the separating fragments. In the C−O range of 1.4−2.8 Å (Figure 7), the absolute value of the negative charge on **OAc** monotonically increases to more than 0.9. The heterolytic nature of the dissociations is unambiguously confirmed by the Mulliken, Löwdin, and NBO charges, as well as at the higher level of theory (def2-TZVPPD). Furthermore, the long-range corrected LC-BLYP functional, which normally gives correct charges for the challenging alkali halide dissociations, likewise gives ca. ± 1.0 NBO charges on the separating fragments. This effectively confirms that at the C−O distance of ca. 2.8 Å, the separating fragments form an intermediate carbocation/acetate contact ionic pair.

The optimized structures and harmonic frequencies of radicals and ions are given in the SI (Table S5). All the radicals and carbocations are locally planar, and the $H_2C\bullet$ (or H_2C^+) moiety is coplanar with the vicinal phenyl rings (δ(H−C−C_{Phe}−C_{Phe}) = 0°). There is no clear-cut radical center, as the radical SOMO is in all cases delocalized over both phenyl rings. This probably accounts for the unreactivity of these benzyl radicals with O_2, and somewhat slower reactivity with TEMPO.

We next compare the energies along the dissociation curves with the energies of the independent (infinitely separated) radicals and ions in the ground and first excited states (Table 5). This reveals that the **OAc** dissociations converge toward the separated ions such that the carbocations are in the S_1 state and the acetate anion is in the ground state. One exception is **p,m-OAc**, where the C−O dissociation runs into an earlier S_1/S_0 conical intersection (hence the bump at ca. 2.5 Å in the **p,m-OAc** dissociation curve), after which the separating fragments converge to the ground-state ions. We note that, owing to the Coulomb attraction, the ionic contact pairs are lower in energy than the infinitely separated ions. The diminishing slope of the dissociation curves indeed suggests a postscission minimum around 3 Å, corresponding to the carbocation/OAc^- ionic pair (Figure 7).

Based on the features of these dissociation curves, we can infer two factors that control the overall photohydrolytic reactivity: (1) the height of the barrier for the C−O bond scission in the S_1 state (Table 5); and (2) the properties of the S_1 dissociation curve following the C−O bond scission, in particular, the steepness of its descent, which determines the probability of recombination of the emerging ion (or radical) pair. Thus, if, in this postscission region, the curve is too flat, potentially even exhibiting a shallow minimum, as is the case for **p,p'-OAc** (Figure 7), the recombination probability should be higher because the lifetime of the contact ion (or radical) pair is longer. Consequently, despite the lowest barrier for the C−O scission (Table 5), **p,p'-OAc** undergoes recombination much more frequently than the remaining isomers causing its photohydrolytic quantum yield to be very small. On the other hand, if the postscission descent is steep, the contact pair will separate more rapidly, thus reducing the recombination and increasing the photohydrolytic efficiency, as is the case for **o,p'-OAc** and **p,m-OAc**. Such a rationale to account for different efficiencies for the decaging has been described.[60] Compared to the **o,m'-OAc**, **m,m'-OAc** or **p,m'-OAc** isomers, **o,p'-OAc** and **p,m-OAc** in addition, exhibit relatively low barriers, which are in line with their largest photohydrolytic quantum yields (Tables 3 and 5).

Table 5. Barriers for the C−O Scission (kcal mol^{-1}), Mulliken and Löwdin Charges on the Atoms of the Rupturing C−O Bond and Their Differences (Δ), and Mayer Bond Orders (MBO) Computed at the S_1 Minimum Geometries[a]

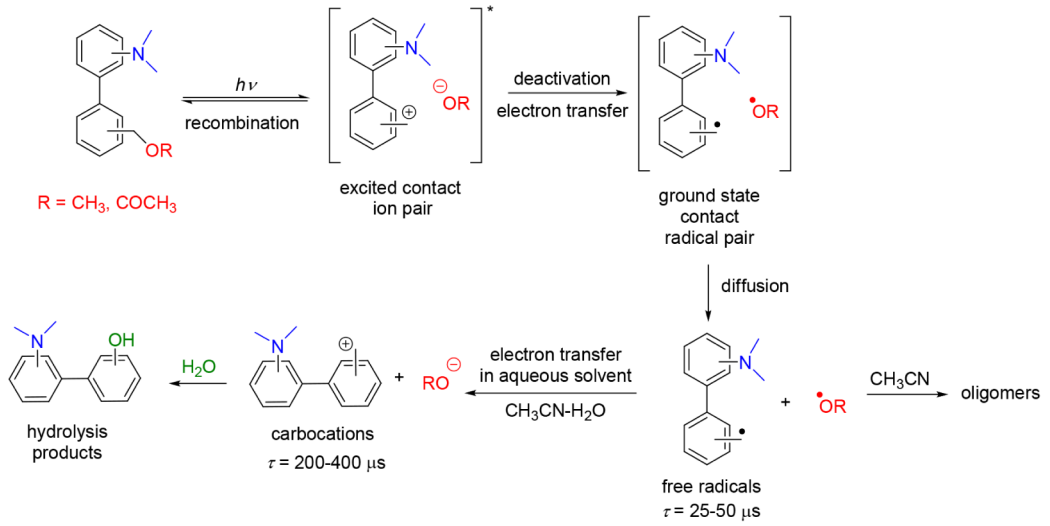
		p,m-OAc	*syn*-o,m'-OAc	*anti*-o,m'-OAc	o,p'-OAc	p,m'-OAc	p,p'-OAc	m,m'-OAc	m,p'-OAc
Barrier		7.1	16.4	15.3	10.1	12.7	6.9	19.6	10.5
Mulliken (S_1)	C	1.67	1.63	1.29	1.14	1.40	1.21	1.76	1.26
	O	−0.61	−0.82	−0.55	−0.53	−0.57	−0.55	−0.68	−0.53
Δ		2.28	2.45	1.84	1.67	1.96	1.76	2.45	1.80
Löwdin (S_1)	C	0.140	0.146	0.139	0.136	0.138	0.134	0.138	0.136
	O	−0.282	−0.286	−0.283	−0.284	−0.284	−0.285	−0.290	−0.284
Δ		0.422	0.433	0.422	0.420	0.422	0.420	0.429	0.419
MBO (S_1)		0.732	0.751	0.716	0.766	0.738	0.738	0.794	0.744
$BACH_2^+$ (S_1) + OAc^- (S_0)		60.9	30.3	32.7	40.8	33.2	53.4	35.8	40.8
$BACH_2\bullet$* + $OAc\bullet$ (D_0)[b]		99.2	88.3	90.3	91.3	84.8	95.2	92.3	87.5
$BACH_2\bullet$ (D_0) + $OAc\bullet$*[b]		63.3	44.7	45.6	51.6	44.9	57.4	44.1	48.4
$BACH_2\bullet$ (D_0) + $OAc\bullet$ (D_0)		41.7	23.1	24.0	30.0	23.3	35.8	22.5	26.8

[a]Furthermore, energies (kcal mol^{-1}) of various infinitely separated ionic and radical pairs relative to the energy of the ground state ionic pair (BA = biphenylamine). [b]Spin-unrestricted theory was used for all the open-shell species. Thus, owing to spin contamination, it is difficult to assign definite multiplicities to the lowest excited states of radical species. For this reason, we designate these states with an asterisk (*).

https://doi.org/10.1021/acs.joc.6c00228
J. Org. Chem. 2026, 91, 5947−5968

Downloaded from pubs.acs.org/joceah/article-pdf/91/17/5947/6205059/acs.joc.6c00228.pdf by RUDJER BOSKOVIC INST user on 05 October 2026

Scheme 7. Mechanism of the Photochemical Elimination Reaction from Biphenylamine Photocages



Considering these two factors, the question now arises why **p,m-OAc** has lower photohydrolytic yields than **o,p'-OAc** despite the lower barrier for the C−O scission and the very steep postscission descent. The likely reason is in dynamical factors associated with the sterically hindered OAc elimination when the amino group and $-CH_2OAc$ substituent share the same ring. Indeed, computing the **p,m-OAc** dissociation curve took the longest, owing to major conformational adjustments required to mitigate the unfavorable steric clashes en route. To avoid the emerging R-CH_2^+ carbocation coplanar with the phenyl ring, the vicinal amino group had to position itself fully perpendicularly to the ring (δ(C−N−C_{Phe}−C_{Phe}) = 90°). Conversely, in **o,p'-OAc** and other isomers where the amino and $-CH_2OAc$ groups reside on different phenyl rings, the release of OAc is unhindered.

Overall, the present computations offer an explanation of the photohydrolytic reactivity of the **OAc** isomers in terms of the properties of the corresponding C−O dissociation curves in the S_1 state. All such curves are uniformly consistent with the heterolytic photolysis of the H_2C−OAc bond and, as such, give no indication of the experimentally observed long-lived radical species (Figures 4 and 6). To account for these radicals, one has to assume that in some stage R-H_2C•···•OAc radical pair can be formed from the R−H_2C^+···$^-$OAc ionic pair. Such a polar-to-radical crossover implies electron transfer from acetate to the carbocation, possibly triggered by the de-excitation from S_1 to S_0. Namely, while the separated D_0 radicals are considerably higher in energy than the separated S_0 ions, they are still lower than the S_1 ionic pair. Consequently, in the course of the relaxation of the ionic pair from the S_1 excited to the ground state, the system may visit potential surface regions that are (nearly) degenerate with the ground-state radical pair. In such an intermediary region, the probability of electron transfer and ion-to-radical interconversion would be the largest; hence, the radical transients could form in sufficient quantities to be detected. Finally, we note that the excited-state radical pairs, such as $BACH_2$•*/OAc•(D_0) or $BACH_2$•(D_0)/OAc•* are too high in energy relative to the S_1 ionic pair and thus inaccessible (Table 5).

Focusing on the **OAc** isomers, which have presently not been synthesized, the photohydrolysis of **m,p'-OAc** is anticipated to be as efficient as that of **o,p'-OAc** because of the great overall similarity of their dissociation curves. In contrast, **m,m'-OAc**, despite the steep postscission descent of its dissociation curve (Figure 7), should be largely inefficient as a photocage owing to by far the highest predicted barrier for the C−O scission (Table 5).

A question of interest is whether the photohydrolytic reactivity of the **OAc** photocages could somehow be anticipated from simpler predictors to circumvent the lengthy computations of the dissociation curves. We here focus on the properties of the S_1 minimum structures as the reactants. The barrier to the C−O scission is found to be smaller if the conformation of the methylene H atoms of $-H_2C$-OAc with respect to the adjacent phenyl ring is eclipsed rather than staggered. Moreover, in the eclipsed conformation, the interaction of the phenyl ring π with the σ^*(C−O) density is visible in the LUMO, which softens the C−O bond. Furthermore, for the photocages with $-CH_2OAc$ and $-NMe_2$ on different rings, there is some correlation with Mulliken atomic charges. In more efficient photocages, the rupturing C−O bond is initially more covalent (i.e., less polarized), as quantified by the difference in the C and O atomic charges (Table 5). The same correlation with the Löwdin charges is more subtle, i.e., more significant figures are needed (Table 5). Regarding Mayer's bond orders, we note that although the CH_2−OAc bonds are tangibly weakened in the S_1 minima (bond order is on average 0.75), the correlation to the observed photohydrolytic efficiency is poor (Table 5). Overall, while the barrier heights can be qualitatively anticipated from several less expensive predictors, the same is not true of the postscission behavior of the dissociation curves. The latter crucially decides on the unexpectedly low photoreaction efficiency of the **p,p'-OAc** isomer.

Finally, we briefly analyze the properties of the dissociation curves corresponding to the three **OH** (**o,p'-OH**, **p,m'-OH**, and **p,p'-OH**) and **OMe** (**o,p'-OMe**, **p,m'-OMe**, and **p,p'-OMe**) isomers (Figure S91 in the SI). The predicted barrier heights for these leaving groups are on average larger by 16 (**OH**) and 18 (**OMe**) kcal mol^{-1} than for the corresponding **OAc** isomers, which is in accord with their modest photohydrolytic reactivity. All three **OMe** dissociation curves begin as heterolytic but, following the S_2/S_1 intersection around the 2.0−2.2 Å C−O distance, abruptly turn homolytic

https://doi.org/10.1021/acs.joc.6c00228
J. Org. Chem. 2026, 91, 5947−5968

Downloaded from pubs.acs.org/joceah/article-pdf/91/17/5947/6205059/acs.joc.6c00228.pdf by RUDJER BOSKOVIC INST user on 05 October 2026

(Figure S91). It is surprising that **p,m'-OMe** is the most photoreactive despite the highest barrier to the photoscission of the CH_2−OMe bond (29.9 kcal mol^{-1}); however, it is notable that this particular isomer has the earliest onset of the intersection seam, around 2.0 Å. Regarding the **OH** derivatives, a similar scenario is seen with **p,p'-OH**, whereas both **o,p'-OH** and **p,m'-OH** dissociate fully heterolytically, which is clearly reflected in the shape of their dissociation curves.

Photochemical Reaction Mechanisms

Based on computational studies, preparative irradiations, fluorescence measurements, and LFP experiments, the photochemical reaction mechanism is proposed. Upon excitation of molecules, singlet excited states are populated that exhibit larger dipole moments compared to the ground state, as indicated from fluorescence measurements. The polarization of molecule imposed by the electron-donating activating amino group is a prerequisite for the cleavage, which takes place heterolytically, giving the contact ion pair (Scheme 7). The efficiency of the photocleavage is governed by the energy barrier for the CH_2−O bond cleavage, as well as the steepness of the potential energy surface after the barrier, which is decisive in determining the ratio of ion recombination to their separation. The deactivation of the ions to the S_0 is accompanied by the ion→radical crossover, since radicals in D_0 are lower in energy compared to ions in S_1. The escape of the benzyl radical from the solvent cage gives rise to free benzyl radicals that were detected by LFP with lifetimes of 25−50 μs. The radicals may also decay by recombination, regenerating the starting material, or undergo recombination and oligomerization in the CH_3CN solution, giving high molecular weight products. Note that the radicals were detected by LFP in both CH_3CN and the aqueous solution, but the longer-lived cations (τ > 200 μs) were observed in the aqueous solution only. It is proposed that the cations and the leaving groups in the form of anions were formed by another electron transfer, which may take place only in aqueous solvent, in the tight or solvent-separated radical pair. Formation of carbocations is indicated from the LFP measurements, but also from the irradiation experiments. In particular, the formation of **p,m'-NHAc** is the typical photoproduct due to the reaction of **p,m'-cat** with CH_3CN and subsequent hydrolysis.

The reactivity pattern for the aminobiphenyls that have the amino activating group and the leaving group in the same ring follows the typical *ortho-meta*-effect in photochemistry. The most efficient hydrolysis reactions occur in cases where the leaving group is in the *ortho*- or *meta*-position to the amino group. On the contrary, the reactivity of aminobiphenyls with the amino group in one ring and the leaving group in other, cannot be straightforwardly connected to the *ortho-meta*-effect. To unravel the reasons for their different reactivity, potential energy surfaces have to be examined, since simple computational parameters (such as computed charges or LUMO orbitals) cannot provide a rationale for their different reactivity.

In Vitro Evaluation of Cell Viability in Cancer Cell Lines

For the application of photocages in biology, it is important to assess their cytotoxicity. Therefore, the influence on cell viability was investigated by a standard MTT assay on selected aminobiphenyls: **p,m-OAc**, **o,m'-OAc**, **o,p'-OAc** and **p,m'-OAc** against three human cancer cell lines HCT116 (colon carcinoma), H460 (lung carcinoma), and MCF-7 (breast carcinoma). The cells were treated with the compounds and either irradiated (3 × 10 min, 350 nm) or kept in the dark (for details, see the SI, Table S6). As a positive control, trioxalene was used, as it is known to induce DNA cross-linking and photocytotoxicity. The selected compounds showed no activity in the dark against HCT116 and H460 and exhibited modest micromolar activity against MCF-7. Upon irradiation, the activity was slightly enhanced, but the IC_{50} values remained above 10 μM in all cases, making the compounds suitable for use in biological systems.

CONCLUSIONS

Differently substituted biphenylamine photocages for the release of alcohols and carboxylic acids were investigated. The esters undergo more efficient photohydrolysis than ethers. The highest value for the quantum yield for the elimination of acetic acid was observed for **o,p'-OAc**, Φ_R = 0.37, and the Φ_R trend follows the sequence **o,p'-OAc** > **p,m-OAc** > **p,m'-OAc** ≈ **o,m'-OAc**, which cannot be explained by simple and well-known *ortho-meta*-effect in photochemistry. To explain the differences in Φ_R, examining the potential energy surfaces for the CH_2−O bond cleavage is necessary. The mechanism of the photoelimination follows the heterolytic cleavage on the singlet excited state surface, giving contact ion pairs. The deactivation to the S_0 is accompanied by polar-to-radical crossover, giving radical pairs and free radicals, which were detected by LFP. Another subsequent electron transfer, occurring in aqueous solvent only, delivers benzyl cations and acetate leaving groups. The applicability of biphenylamine photocages in organic synthesis was demonstrated by the photoelimination of palmitic acid and benzoic acid in high isolable yields from the corresponding esters. The photochemical reactivity presented herein is important for the general knowledge on the effects that govern the photochemical reactivity of molecules in excited states. Moreover, it is important in the rational design of the next generation of biphenylamine photocages, that could be excited in two-photon processes, and thus will be applicable in biological systems.

EXPERIMENTAL SECTION

General

Solvents and reagents were obtained from commercial suppliers and used without further purification unless otherwise noted. Solvents for chromatographic separations were used as delivered (p.a. or HPLC grade) or purified by distillation. Column chromatography was carried out using silica gel (0.063−0.2 nm). Organic layers were dried over anhydrous $MgSO_4$ after extraction. ^1H and ^{13}C NMR spectra were measured on spectrometer at 600 and 300 MHz for ^1H, and at 150 and 75 MHz for ^{13}C nuclei. Chemical shifts are reported in ppm using tetramethylsilane (TMS) as a reference. HRMS analyses were performed on an Agilent 6545 Q-TOF instrument. Irradiations were conducted in a Luzchem photochemical reactor (8 lamps, 300 or 350 nm, 1 lamp 8W) using quartz test tubes positioned in the center of the reactor, 15 cm from the lamps. Large-scale irradiations were performed in a Rayonet photochemical reactor equipped with 10 lamps with the output at 300 nm (1 lamp 8 W), in a Pyrex vessel (diameter 6 cm) centered in the middle of the reactor, 10 cm away from the lamps. During the irradiation, the solution was cooled by a finger tap-H_2O condenser and purged by a stream of Ar. The following abbreviations were used: DIPEA - *N,N*-Diisopropylethylamine, br s—broad singlet, d—doublet, t—triplet, q—quartet, dd—doublet of doublets, m—multiplet, rt—room temperature.

Downloaded from pubs.acs.org/joceah/article-pdf/91/17/5947/6205059/acs.joc.6c00228.pdf by RUDJER BOSKOVIC INST user on 05 October 2026

https://doi.org/10.1021/acs.joc.6c00228
J. Org. Chem. 2026, 91, 5947−5968

Caution! ultraviolet light is damaging to biological tissues. Caution is required when working with lamps, and protective eyewear must always be used.

General Procedure for Methylation

Amine (5.8 mmol, 1 equiv) and Na_2HPO_4 (**5** and **6**: 20.3 mmol, 3.5 eq or **1**, **7**, and **8**: 34.9 mmol, 6 equiv) were suspended in anhydrous DMF (30 mL). Methyl iodide (**5** and **6**: 17.4 mmol, 3 eq or **1**, **7**, and **8**: 34.9 mmol, 6 equiv) was added, and the reaction mixture was stirred at room temperature overnight under a nitrogen atmosphere. The next day, the reaction mixture was diluted with water (100 mL) (or 1 M NaOH), ensuring that the pH remained above 7, and extracted with ethyl acetate (3 × 30 mL). The combined organic layers were washed with brine (2 × 15 mL) and H_2O (1 × 20 mL), then dried over anhydrous $MgSO_4$. After filtration, the solvent was removed on a rotary evaporator. The purification of the product was conducted by column chromatography on silica gel using *n*-hexane/CH_2Cl_2.

Caution! *n*-Hexane is a flammable liquid that causes skin irritation and reproductive toxicity. Care should be taken when handling the substance, which should be done in a fume hood. Protective eyewear and gloves should be worn.

Caution! CH_2Cl_2 is a carcinogenic substance and causes skin and eye irritation. Care should be taken when handling the substance, which should be done in a fume hood. Protective eyewear and gloves should be worn.

(5-Bromo-2-(dimethylamino)phenyl)methanol (5). The synthesis was carried out according to the general procedure for methylation. To the suspension of compound **3** (670 mg, 3.3 mmol) and Na_2HPO_4 (1.7 g, 11.6 mmol) in anhydrous DMF (20 mL), methyl iodide (620 μL, 10.1 mmol) was added. After the extraction workup, the crude product was purified by column chromatography on silica gel using *n*-hexane/CH_2Cl_2 (2:1) as the eluent to afford 580 mg (76%) of pure product **5** in the form of colorless powder.

5: mp 83−84 °C, ^{1}H NMR ($CDCl_3$, 300 MHz): δ 7.40−7.31 (m, 2H), 7.06 (d, 1H, *J* = 8.3 Hz), 5.01 (br s, 1H), 4.75 (s, 2H), 2.69 (s, 6H); ^{13}C{1H} NMR ($CDCl_3$, 75 MHz): δ 151.0, 137.8, 131.3, 131.0, 121.8, 117.3, 64.0, 44.6 (2C); HRMS (LC-Q/TOF) *m*/*z* [M + H]$^+$ Calcd for $C_9H_{13}BrNO^+$ 230.0175; Found 230.0186.

(3,5-Dibromo-2-(dimethylamino)phenyl)methanol (6). The synthesis was carried out according to the general procedure for methylation. To the suspension of compound **4** (302 mg, 1.1 mmol) and Na_2HPO_4 (536 mg, 3.8 mmol) in anhydrous DMF (8 mL), methyl iodide (200 μL, 3.2 mmol) was added. After extraction and workup, the crude product was purified by column chromatography on silica gel using *n*-hexane/CH_2Cl_2 (2:1) as the eluent to afford 80 mg (24%) of pure product **6** in the form of a colorless powder.

6: mp 92−93 °C, ^{1}H NMR ($CDCl_3$, 600 MHz): δ 7.61 (d, 1H, *J* = 2.3 Hz), 7.36 (d, 1H, *J* = 2.3 Hz), 4.67 (s, 2H), 3.85 (br s, 1H), 2.87 (s, 6H); ^{13}C{1H} NMR ($CDCl_3$, 75 MHz): δ 147.3, 143.9, 135.7, 130.4, 123.5, 119.7, 63.8, 42.1 (2C); HRMS (LC-Q/TOF) *m*/*z* [M + H]$^+$ Calcd for $C_9H_{12}Br_2NO^+$ 307.9280; Found 307.9277.

General Procedure for Suzuki-Miyaura Cross-Coupling Reaction

Methanol solution (6 mL) of phenylboronic acid or 3- or 4-formylphenylboronic acid (1.0 mmol, 1 eq; except in the preparation of **p,m-OH-m-Ph**: 2.0 mmol, 2 equiv) and a toluene solution (12 mL) of bromo derivative (**1** or **5**−**8**, 1.0 mmol, 1 equiv) were combined. To the mixture were added anhydrous potassium carbonate (2 mmol, 2 equiv) and tetrakis(triphenylphosphine) palladium $Pd(PPh_3)_4$ (0.02 mol, 0.02 equiv), and the reaction mixture was heated in an oil bath at reflux for 24 h. The next day, the cooled mixture was diluted with water (30 mL), and the layers were separated. The aqueous layer was extracted with CH_2Cl_2 (3 × 20 mL), and the combined organic layers were dried over anhydrous $MgSO_4$. After filtration, the solvent was removed on a rotary evaporator, and the crude product was purified by column chromatography on silica gel to afford products **9**−**12**, **p,m-OH**, and **p,m-OH-m-Ph**.

2′-(Dimethylamino)-[1,1′-biphenyl]-3-carbaldehyde (9). The reaction was carried out according to the general procedure for the Suzuki-Miyaura cross-coupling reaction using a methanol solution (6 mL) of 3-formylphenylboronic acid (146 mg, 1.0 mmol), a toluene solution (12 mL) of compound **7** (200 mg, 1.0 mmol), anhydrous potassium carbonate (276.0 mg, 2.0 mmol), and tetrakis-(triphenylphosphine)palladium $Pd(PPh_3)_4$ (23 mg, 0.02 mmol). The product was purified by column chromatography on silica gel using *n*-hexane/CH_2Cl_2 (1:1) as the eluent to afford 115 mg (52%) of pure product **9** in the form of yellow oil.

9: ^{1}H NMR ($CDCl_3$, 300 MHz): δ 10.05 (s, 1H), 8.09 (s, 1H), 7.89 (d, 1H, *J* = 7.6 Hz), 7.82 (d, 1H, *J* = 7.6 Hz), 7.55 (t, 1H, *J* = 7.6 Hz), 7.36−7.27 (m, 1H), 7.26−7.20 (m, 1H), 7.09−7.02 (m, 2H), 2.54 (s, 6H); ^{13}C{1H} NMR ($CDCl_3$, 75 MHz): δ 192.6, 151.3, 142.9, 136.7, 134.9, 132.8, 131.5, 130.3, 129.0, 128.8, 127.7, 121.9, 118.0, 43.5 (2C); HRMS (LC-Q/TOF) *m*/*z* [M + H]$^+$ Calcd for $C_{15}H_{16}NO^+$ 226.1226; Found 226.1237.

2′-(Dimethylamino)-[1,1′-biphenyl]-4-carbaldehyde (10). The reaction was carried out according to the general procedure for the Suzuki-Miyaura cross-coupling reaction using a methanol solution (3 mL) of 4-formylphenylboronic acid (73 mg, 0.5 mmol), a toluene solution (6 mL) of compound **7** (100 mg, 0.5 mmol), anhydrous potassium carbonate (135.0 mg, 1.0 mmol), and tetrakis-(triphenylphosphine)palladium $Pd(PPh_3)_4$ (11 mg, 0.01 mmol). The product was purified by column chromatography on silica gel using *n*-hexane/CH_2Cl_2 (1:1) as the eluent to afford 54 mg (48%) of pure product **10** in the form of yellow oil.

10: ^{1}H NMR ($CDCl_3$, 300 MHz): δ 10.04 (s, 1H), 7.91 (d, 2H, *J* = 8.3 Hz), 7.77 (d, 2H, *J* = 8.3 Hz), 7.37 − 7.28 (m, 1H), 7.22 (d, 1H, *J* = 8.6 Hz), 7.08−7.01 (m, 2H), 2.55 (s, 6H); ^{13}C{1H} NMR ($CDCl_3$, 75 MHz): δ 191.0, 150.3, 147.6, 133.6, 131.5, 130.5, 128.9 (2C), 128.2 (2C), 128.0, 120.6, 116.8, 42.5 (2C); HRMS (LC-Q/TOF) *m*/*z* [M + H]$^+$ Calcd for $C_{15}H_{16}NO^+$ 226.1226; Found 226.1237.

(4-(Dimethylamino)-[1,1′-biphenyl]-3-yl)methanol (p,m-OH). The reaction was carried out according to the general procedure for the Suzuki-Miyaura cross-coupling reaction using a methanol solution (5 mL) of phenylboronic acid (111 mg, 0.9 mmol), a toluene solution (10 mL) of compound **5** (210 mg, 0.9 mmol), anhydrous potassium carbonate (251.0 mg, 1.8 mmol), and tetrakis-(triphenylphosphine)palladium $Pd(PPh_3)_4$ (21 mg, 0.02 mmol). The product was purified by column chromatography on silica gel using *n*-hexane/CH_2Cl_2 (1:1) as the eluent to afford 176 mg (85%) of pure product **p,m-OH** in the form of colorless oil.

p,m-OH: ^{1}H NMR ($CDCl_3$, 600 MHz): δ 7.57−7.55 (m, 2H), 7.49 (dd, 1H, *J* = 8.3, 2.2 Hz), 7.45− 7.40 (m, 3H), 7.33 (dd, 1H, *J* = 8.6, 1.6 Hz), 7.28 (d, 1H, *J* = 8.3 Hz), 5.43 (br s, 1H), 4.89 (s, 2H), 2.77 (s, 6H); ^{13}C{1H} NMR ($CDCl_3$, 75 MHz): δ 151.1, 140.6, 137.4, 135.4, 128.8 (2C), 127.3, 127.1, 127.0 (2C), 126.8, 120.4, 65.0, 44.7 (2C); UV (CH_3CN) λ_{max}/nm (ε/dm^3 mol^{-1} cm^{-1}) = 279 (11900); HRMS (LC-Q/TOF) *m*/*z* [M + H]$^+$ Calcd for $C_{15}H_{18}NO^+$ 228.1383; Found 228.1386.

2′-(Dimethylamino)-[1,1′-biphenyl]-4-carbaldehyde (p,m-OH-m-Ph). The reaction was carried out according to the general procedure for the Suzuki-Miyaura cross-coupling reaction using a methanol solution (5 mL) of phenylboronic acid (146 mg, 1.2 mmol), a toluene solution (10 mL) of compound **6** (191 mg, 0.6 mmol), anhydrous potassium carbonate (171.0 mg, 1.7 mmol), and tetrakis(triphenylphosphine)palladium $Pd(PPh_3)_4$ (28 mg, 0.02 mmol). The product was purified by column chromatography on silica gel using *n*-hexane/CH_2Cl_2 (1:1) as the eluent to afford 69 mg (37%) of pure product **p,m-OH-m-Ph** in the form of colorless oil.

p,m-OH-m-Ph: ^{1}H NMR ($CDCl_3$, 600 MHz): δ 7.59 (dd, 2H, *J* = 8.3, 1.1 Hz), 7.50 (d, 1H, *J* = 2.3 Hz), 7.45−7.30 (m, 9H), 4.88 (s, 2H), 4.50 (s, 1H), 2.56 (s, 6H); ^{13}C{1H} NMR ($CDCl_3$, 150 MHz): δ 147.6, 141.8, 141.2, 140.3, 138.6, 137.2, 130.0, 129.4 (2C), 128.7 (2C), 128.0 (2C), 127.2, 127.2, 127.0 (2C), 126.5, 64.9, 44.1 (2C); UV (CH_3CN) λ_{max}/nm (ε/dm^3 mol^{-1} cm^{-1}) = 300 (9813); HRMS (LC-Q/TOF) *m*/*z* [M + H]$^+$ Calcd for $C_{21}H_{22}NO^+$ 304.1696; Found 304.1699.

Downloaded from pubs.acs.org/joceah/article-pdf/91/17/5947/6205059/acs.joc.6c00228.pdf by RUDJER BOSKOVIC INST user on 05 October 2026

https://doi.org/10.1021/acs.joc.6c00228
J. Org. Chem. 2026, 91, 5947−5968

General Procedure for Reduction with $NaBH_4$

A solution of aldehyde **2** or **9**–**12** (1 mmol, 1 eq) in ethanol (5 mL) was cooled to 0 °C in an ice bath, and $NaBH_4$ (1.5 mmol, 1.5 equiv) was then added in small proportions. After the mixture was stirred for 2 h at room temperature, water (10 mL) was added while maintaining the temperature at 0 °C in the ice bath. The reaction mixture was extracted with ethyl acetate (3 × 15 mL), the combined extracts were dried over anhydrous $MgSO_4$, filtered, and the solvent was removed under reduced pressure. The product was purified by column chromatography on silica gel using *n*-hexane/CH_2Cl_2 (1:1) as the eluent to afford pure products.

(6-(Dimethylamino)-[1,1′-biphenyl]-3-yl)methanol (o,m-OH). The reaction was carried out according to the general procedure for reduction with $NaBH_4$ using a suspension of compound **2** (600 mg, 2.7 mmol) and $NaBH_4$ (151 mg, 4.1 mmol) in ethanol (15 mL). The crude product was purified by column chromatography on silica gel using *n*-hexane/CH_2Cl_2 (1:1) as the eluent to affording pure product **o,m-OH** (400 mg, 66%) in the form of yellow oil.

o,m-OH: ^{1}H NMR (CD_3OD, 300 MHz): δ 7.59–7.51 (m, 2H), 7.43–7.34 (m, 2H), 7.32–7.22 (m, 2H), 7.18 (d, 1H, J = 2.2 Hz), 7.06 (d, 1H, J = 8.2 Hz), 4.56 (s, 2H), 2.51 (s, 6H); ^{13}C{1H} NMR (CD_3OD, 150 MHz): δ 150.5, 141.9, 134.3, 134.3, 130.4, 128.3 (2C), 127.9 (2C), 126.7, 126.2, 117.3, 63.6, 42.4 (2C); UV (CH_3CN) λ_{max}/nm (ε/dm^3 mol^{-1} cm^{-1}) = 310 (2480); HRMS (LC-Q/TOF) m/z [M + H]$^+$ Calcd for $C_{15}H_{18}NO^+$ 228.1383; Found 228.1390.

(2′-(Dimethylamino)-[1,1′-biphenyl]-3-yl)methanol (o,m′-OH). The reaction was carried out according to the general procedure for reduction with $NaBH_4$ using a suspension of compound **9** (180 mg, 0.8 mmol) and $NaBH_4$ (45 mg, 1.2 mmol) in ethanol (6 mL). The crude product was purified by column chromatography on silica gel using *n*-hexane/CH_2Cl_2 (1:1) as the eluent, affording pure product **o,m′-OH** (132 mg, 73%) in the form of colorless oil.

o,m′-OH: ^{1}H NMR ($CDCl_3$, 600 MHz): 7.56 (s, 1H), 7.53 (d, 1H, J = 7.7 Hz), 7.39 (t, 1H, J = 7.6 Hz), 7.31 (d, 1H, J = 7.6 Hz), 7.29–7.26 (m, 1H), 7.22 (dd, 1H, J = 7.5, 1.5 Hz), 7.04 (d, 1H, J = 8.1 Hz), 7.01 (t, 1H, J = 7.4 Hz), 4.74 (s, 2H), 2.54 (s, 6H); ^{13}C{1H} NMR ($CDCl_3$, 75 MHz) δ 141.1, 134.0, 131.8, 128.6, 128.3, 128.0, 127.3, 125.3, 121.8, 117.8, 65.5, 43.7 (2C); UV (CH_3CN) λ_{max}/nm (ε/dm^3 mol^{-1} cm^{-1}) = 270 (4500); HRMS (LC-Q/TOF) m/z [M + H]$^+$ Calcd for $C_{15}H_{18}NO^+$ 228.1383; Found 228.1394.

(2′-(Dimethylamino)-[1,1′-biphenyl]-4-yl)methanol (o,p′-OH). The reaction was carried out according to general procedure for reduction with $NaBH_4$ using a suspension of compound **10** (180 mg, 0.8 mmol) and $NaBH_4$ (45 mg, 1.2 mmol) in ethanol (6 mL). The crude product was purified by column chromatography on silica gel using *n*-hexane/CH_2Cl_2 (1:1) as the eluent, affording pure product **o,p′-OH** (153 mg, 84%) in the form of colorless oil.

o,p′-OH: ^{1}H NMR ($CDCl_3$, 300 MHz): δ 7.59 (d, 2H, J = 8.0 Hz), 7.40 (d, 2H, J = 8.0 Hz), 7.30– 7.21 (m, 2H), 7.06–6.99 (m, 2H), 4.74 (s, 2H), 2.55 (s, 6H); ^{13}C{1H} NMR ($CDCl_3$, 75 MHz): δ 151.3, 141.5, 139.0, 133.8, 131.7, 128.9 (2C), 128.1, 127.1 (2C), 121.5, 117.7, 65.3, 43.4 (2C); UV (CH_3CN) λ_{max}/nm (ε/dm^3 mol^{-1} cm^{-1}) = 280 (3650); HRMS (LC-Q/TOF) m/z [M + H]$^+$ Calcd for $C_{15}H_{18}NO^+$ 228.1383; Found 228.1387.

(4′-(Dimethylamino)-[1,1′-biphenyl]-3-yl)methanol (p,m′-OH). The reaction was carried out according to the general procedure for reduction with $NaBH_4$ using a suspension of compound **11** (212 mg, 0.9 mmol) and $NaBH_4$ (53 mg, 1.4 mmol) in ethanol (10 mL). The crude product was purified by column chromatography on silica gel using *n*-hexane/CH_2Cl_2 (1:1) as the eluent, affording pure product **p,m′-OH** (201 mg, 94%) in the form of colorless oil.

p,m′-OH: ^{1}H NMR ($(CD_3)_2CO$, 300 MHz): δ 7.60 (s, 1H), 7.53 (d, 2H, J = 8.8 Hz), 7.47 (d, 1H, J = 7.7 Hz), 7.35 (t, 1H, J = 7.6 Hz), 7.25 (d, 1H, J = 7.7 Hz), 6.84 (d, 2H, J = 8.6 Hz), 4.68 (d, 2H, J = 5.6 Hz), 4.20 (t, 1H, J = 5.6 Hz), 2.99 (s, 6H); ^{13}C{1H} NMR ($(CD_3)_2CO$, 75 MHz): δ 151.1, 143.8, 141.9, 129.6, 129.4, 128.2 (2C), 125.2, 125.1, 125.0, 113.6 (2C), 64.9, 40.6 (2C); UV (CH_3CN) λ_{max}/nm (ε/dm^3 mol^{-1} cm^{-1}) = 270 (8990); HRMS (LC-Q/TOF) m/z [M + H]$^+$ Calcd for $C_{15}H_{18}NO^+$ 228.1383; Found 228.1391.

General Procedure for the Preparation of Ethers

An alcohol (1 mmol, 1 eq) was dissolved in dry CH_2Cl_2 (6 mL), cooled to 0 °C in an ice bath, and $SOCl_2$ was added (1.8 mmol, 1.8 eq; except in the preparation of **p,m-OMe-m-Ph**: 3.6 mmol, 3.6 equiv). The mixture was stirred at 0 °C for 20 min and then at room temperature for 20 h. The solvent was removed on a rotary evaporator, and the chloride products were used in the next step without purification.

To a solution of the chloride (1 mmol, 1 eq) in anhydrous methanol (5.6 mL), a freshly prepared solution of sodium methoxide was added dropwise. The sodium methoxide solution was prepared by reacting Na (3 mmol, 3 eq; except in the preparation of **p,m-OMe-m-Ph**: 6 mmol, 6 equiv) in anhydrous methanol (5.6 mL; except in the preparation of **p,m-OMe-m-Ph**: 11.2 mL). The reaction mixture was stirred at room temperature overnight. Methanol was removed on a rotary evaporator, and CH_2Cl_2 (15 mL) was added to dissolve the residue. The reaction mixture was washed with water (15 mL), dried over anhydrous $MgSO_4$, and filtered. The solvent was removed on a rotary evaporator, and the product was purified by column chromatography on silica gel using *n*-hexane/CH_2Cl_2 as the eluent to give ethers.

Caution! $SOCl_2$ is a toxic substance if inhaled, and it causes skin corrosion and serious eye damage. Extreme care should be taken when handling the substance, which should be done in a fume hood. Protective eyewear and gloves should be worn.

Caution! sodium is a substance which, in contact with water, emits flammable gases; it causes skin corrosion and serious eye damage. Care should be taken when handling the substance. Protective eyewear and gloves should be worn.

5-(Methoxymethyl)-*N*,*N*-dimethyl-[1,1′-biphenyl]-2-amine (o,m-OMe). The reaction was carried out according to the general procedure for the preparation of ethers, using a solution of compound **o,m-OH** (150 mg, 0.7 mmol) and $SOCl_2$ (86 μL, 1.2 mmol) in anhydrous CH_2Cl_2 (4 mL). The solvent was removed on a rotary evaporator, and the crude product **o,m-Cl** was used in the next step without isolation.

To a solution of **o,m-Cl** in anhydrous methanol (4 mL), a freshly prepared solution of sodium methoxide (Na, 46 mg, 2.0 mmol in 4 mL anhydrous methanol) was added dropwise. The crude product was purified by column chromatography on silica gel using *n*-hexane/CH_2Cl_2 (2:1) as the eluent to afford pure product **o,m-OMe** (100 mg, 63%) in the form of colorless oil.

o,m-OMe: ^{1}H NMR (CD_3OD, 300 MHz): δ 7.56 (dt, 2H, J = 7.0, 1.8 Hz), 7.37 (td, 2H, J = 7.1, 1.8 Hz), 7.28 (dt, 1H, J = 7.4, 1.4 Hz), 7.25–7.19 (m, 1H), 7.14 (d, 1H, J = 2.0 Hz), 7.04 (d, 1H, J = 8.2 Hz), 4.40 (s, 2H), 3.36 (s, 3H), 2.51 (s, 6H); ^{13}C{^{1}H} NMR (CD_3OD, 75 MHz): δ 152.3, 143.2, 135.6, 132.7, 132.3, 129.7 (2C), 129.4 (2C), 129.1, 127.7, 118.7, 75.5, 58.0, 43.8 (2C); UV (CH_3CN) λ_{max}/nm (ε/dm^3 mol^{-1} cm^{-1}) = 310 (3110); HRMS (LC-Q/TOF) m/z [M + H]$^+$ Calcd for $C_{16}H_{20}NO^+$ 242.1539; Found 242.1551.

3-(Methoxymethyl)-*N*,*N*-dimethyl-[1,1′-biphenyl]-4-amine (p,m-OMe). The reaction was carried out according to the general procedure for the preparation of ethers, using a solution of compound **p,m-OH** (107 mg, 0.5 mmol) and $SOCl_2$ (61 μL, 0.9 mmol) in anhydrous CH_2Cl_2 (3 mL). The solvent was removed on a rotary evaporator, and the crude product **p,m-Cl** was used in the next step without isolation.

To a solution of **p,m-Cl** in anhydrous methanol (2.8 mL), a freshly prepared solution of sodium methoxide (Na, 32 mg, 1.4 mmol in 2.8 mL anhydrous methanol) was added dropwise. The crude product was purified by column chromatography on silica gel using *n*-hexane/CH_2Cl_2 (2:1) as the eluent to afford pure product **p,m-OMe** (33 mg, 29%) in the form of a white powder.

p,m-OMe: mp 53–54 °C, ^{1}H NMR (CD_3OD, 300 MHz): δ 7.63 (d, 1H, J = 2.3 Hz), 7.57 (t, 2H, J = 7.7 Hz), 7.51 (dd, 1H, J = 8.4, 2.4 Hz), 7.40 (t, 2H, J = 7.5 Hz), 7.28 (t, 1H, J = 7.4 Hz), 7.19 (d, 1H, J = 8.4 Hz), 4.60 (s, 2H), 3.44 (s, 3H); 2.73 (s, 6H); ^{13}C{^{1}H} NMR (CD_3OD, 150 MHz): δ 153.3, 142.2, 136.9, 133.4, 129.8 (2C), 129.2, 127.9, 127.8, 127.6 (2C), 120.2, 71.7, 58.6, 45.5 (2C); UV (CH_3CN)

Downloaded from pubs.acs.org/joceah/article-pdf/91/17/5947/6205059/acs.joc.6c00228.pdf by RUDJER BOSKOVIC INST user on 05 October 2026

https://doi.org/10.1021/acs.joc.6c00228
J. Org. Chem. 2026, 91, 5947–5968

λ_{max}/nm (ε/dm^3 mol^{-1} cm^{-1}) = 283 (15400); HRMS (LC-Q/TOF) m/z [M + H]$^+$ Calcd for $C_{16}H_{20}NO^+$ 242.1539; Found 242.1546.

5′-(Methoxymethyl)-*N*,*N*-dimethyl-[1,1′:3′,1″-terphenyl]-4′-amine (p,m-OMe-m-Ph). The reaction was carried out according to the general procedure for the preparation of ethers, using a solution of compound **p,m-OH-m-Ph** (150 mg, 0.5 mmol) and $SOCl_2$ (128 μL, 1.8 mmol) in anhydrous CH_2Cl_2 (4 mL). The solvent was removed on a rotary evaporator, and the crude product **p,m-Cl-m-Ph** was used in the next step without isolation.

To a solution of **p,m-Cl-m-Ph** in anhydrous methanol (4 mL), a freshly prepared solution of sodium methoxide (Na, 68 mg, 2.9 mmol in 8 mL anhydrous methanol) was added dropwise. The crude product was purified by column chromatography on silica gel using *n*-hexane/CH_2Cl_2 (2:1) as the eluent to afford pure product **p,m-OMe-m-Ph** (59 mg, 38%) in the form of colorless oil.

p,m-OMe-m-Ph: ^{1}H NMR ($CDCl_3$, 300 MHz): δ 7.69 (d, 1H, J = 2.1 Hz), 7.61 (d, 2H, J = 7.7 Hz), 7.47−7.23 (m, 9H), 4.61 (s, 2H), 3.49 (s, 3H); 2.55 (s, 6H); ^{13}C{^{1}H} NMR ($CDCl_3$, 75 MHz) δ 148.1, 142.3, 140.7, 140.3, 136.7, 136.3, 129.6, 129.2 (2C), 128.6 (2C), 128.0 (2C), 127.0 (2C), 126.9, 126.7, 126.7, 71.8, 58.6, 44.1 (2C); UV (CH_3CN) λ_{max}/nm (ε/dm^3 mol^{-1} cm^{-1}) = 300 (10468); HRMS (LC-Q/TOF) m/z [M + H]$^+$ Calcd for $C_{22}H_{24}NO^+$ 318.1852; Found 318.1858.

3′-(Methoxymethyl)-*N*,*N*-dimethyl-[1,1′-biphenyl]-2-amine (o,m′-OMe). The reaction was carried out according to the general procedure for the preparation of ethers, using a solution of compound **o,m′-OH** (86 mg, 0.4 mmol) and $SOCl_2$ (51 μL, 0.7 mmol) in anhydrous CH_2Cl_2 (3 mL). The solvent was removed on a rotary evaporator, and the crude product **o,m′-Cl** was used in the next step without isolation.

To a solution of **o,m′-Cl** in anhydrous methanol (2.4 mL), a freshly prepared solution of sodium methoxide (Na, 26 mg, 1.1 mmol in 2.4 mL anhydrous methanol) was added dropwise. The crude product was purified by column chromatography on silica gel using *n*-hexane/CH_2Cl_2 (2:1) as the eluent, affording pure product **o,m′-OMe** (41 mg, 45%) in the form of colorless oil.

o,m′-OMe: ^{1}H NMR (CD_3OD, 600 MHz): δ 7.51 (s, 1H), 7.47 (td, 1H, J = 7.7, 1.5 Hz), 7.37 (t, 1H, J = 7.7 Hz), 7.26 (d, 1H, J = 7.6 Hz), 7.24 (dt, 1H, J = 1.8, 8.3 Hz), 7.16 (dd, 1H, J = 7.52, 1.5 Hz), 7.07 (dd, 1H, J = 8.1, 1.1 Hz), 6.99 (td, 1H, J = 7.4, 1.2 Hz), 4.49 (s, 2H), 3.39 (s, 3H), 2.51 (s, 6H); ^{13}C NMR{^{1}H} (CD_3OD, 150 MHz): δ 152.6, 143.5, 139.4, 135.6, 132.5, 132.4, 129.4, 129.3, 129.3, 129.2, 127.2, 118.8, 75.8, 58.2, 43.8 (2C); UV (CH_3CN) λ_{max}/nm (ε/dm^3 mol^{-1} cm^{-1}) = 270 (4540); HRMS (LC-Q/TOF) m/z [M + H]$^+$ Calcd for $C_{16}H_{20}NO^+$ 242.1539; Found 242.1542.

4′-(Methoxymethyl)-*N*,*N*-dimethyl-[1,1′-biphenyl]-2-amine (o,p′-OMe). The reaction was carried out according to the general procedure for the preparation of ethers, using a solution of compound **o,p′-OH** (90 mg, 0.4 mmol) and $SOCl_2$ (52 μL, 0.7 mmol) in anhydrous CH_2Cl_2 (3 mL). The solvent was removed on a rotary evaporator, and the crude product **o,p′-Cl** was used in the next step without isolation.

To a solution of **o,p′-Cl** in anhydrous methanol (2.4 mL), a freshly prepared solution of sodium methoxide (Na, 28 mg, 1.1 mmol in 2.4 mL anhydrous methanol) was added dropwise. The crude product was purified by column chromatography on silica gel using *n*-hexane/CH_2Cl_2 (2:1) as the eluent, affording pure product **o,p′-OMe** (41 mg, 43%) in the form of colorless oil.

o,p′-OMe: ^{1}H NMR (CD_3OD, 600 MHz): δ 7.53 (d, 2H, J = 8.3 Hz), 7.36 (d, 2H, J = 8.3 Hz), 7.23 (td, 1H, J = 7.7, 1.6 Hz), 7.16 (dd, 1H, J = 7.6, 1.8 Hz), 7.06 (dd, 1H, J = 8.2, 1.1 Hz), 6.98 (td, 1H, J = 7.4, 1.2 Hz), 4.49 (s, 2H), 3.40 (s, 3H), 2.50 (s, 6H); ^{13}C{^{1}H} NMR (CD_3OD, 150 MHz): δ 152.6, 142.9, 137.6, 135.5, 132.4, 129.7 (2C), 129.2, 129.0 (2C), 122.8, 118.9, 75.6, 58.3, 43.8 (2C); UV (CH_3CN) λ_{max}/nm (ε/dm^3 mol^{-1} cm^{-1}) = 274 (6120); HRMS (LC-Q/TOF) m/z [M + H]$^+$ Calcd for $C_{16}H_{20}NO^+$ 242.1539; Found 242.1548.

3′-(Methoxymethyl)-*N*,*N*-dimethyl-[1,1′-biphenyl]-4-amine (p,m′-OMe). The reaction was carried out according to the general procedure for the preparation of ethers, using a solution of compound **p,m′-OH** (100 mg, 0.4 mmol) and $SOCl_2$ (57 μL, 0.8 mmol) in anhydrous CH_2Cl_2 (3 mL). The solvent was removed on a rotary evaporator, and the crude product **p,m′-Cl** was used in the next step without isolation.

To a solution of **p,m′-Cl** in anhydrous methanol (2.6 mL), a freshly prepared solution of sodium methoxide (Na, 30 mg, 1.3 mmol in 2.6 mL dry methanol) was added dropwise. The crude product was purified by column chromatography on silica gel using *n*-hexane/CH_2Cl_2 (2:1) as theeluent to afford pure product **p,m′-OMe** (47 mg, 44%) in the form of colorless powder.

p,m′-OMe: mp 62−63 °C, ^{1}H NMR (CD_3OD, 300 MHz): δ 7.68−7.49 (m, 4H), 7.42 (t, 2H, J = 7.5 Hz), 7.30 (t, 1H, J = 7.3 Hz), 7.21 (d, 1H, J = 8.3 Hz), 4.61 (s, 2H), 3.46 (s, 3H), 2.75 (s, 6H); ^{13}C{1H} NMR (CD_3OD, 150 MHz): δ 151.9, 140.8, 135.5, 132.0, 128.4 (2C), 127.8, 126.5, 126.4, 126.2 (2C), 118.8, 70.4, 57.2, 44.1 (2C); UV (CH_3CN) λ_{max}/nm (ε/dm^3 mol^{-1} cm^{-1}) = 270 (7950); HRMS (LC-Q/TOF) m/z [M + H]$^+$ Calcd for $C_{16}H_{20}NO^+$ 242.1539; Found 242.1536.

General Procedure for the Preparation of Esters

The alcohol (1 mmol, 1 equiv) was dissolved in anhydrous CH_2Cl_2 (5 mL), and then triethylamine (1.2 mmol, 1.2 eq; except in the preparation of **p,m-OAc-m-Ph**: 2.4 mmol, 2.4 equiv) and acetyl chloride (1.2 mmol; except in the preparation of **p,m-OAc-m-Ph**: 2.4 mmol, 2.4 equiv) were added to the solution. The mixture was stirred for 3 h at room temperature. The reaction mixture was diluted with CH_2Cl_2 (15 mL) and washed with brine (15 mL) and water (2 × 10 mL). The organic phase was dried over anhydrous $MgSO_4$ and filtered. The solvent was removed under reduced pressure, and the crude product was purified by column chromatography to yield pure esters.

(6-(Dimethylamino)-[1,1′-biphenyl]-3-yl)methyl acetate (o,m-OAc). The reaction was carried out according to the procedure for the preparation of esters using a solution of **o,m-OH** (150 mg, 0.7 mmol), TEA (110 μL, 0.8 mmol), and AcCl (57 μL, 0.8 mmol) in anhydrous CH_2Cl_2 (4 mL). The crude product was purified by column chromatography on silica gel using *n*-hexane/ethyl acetate (2:1) as the eluent to give pure product **o,m-OAc** (110 mg, 62%) in the form of yellow oil.

o,m-OAc: ^{1}H NMR (CD_3Cl, 300 MHz): δ 7.56 (d, 2H, J = 7.6 Hz), 7.39 (t, 2H, J = 7.6 Hz), 7.33−7.27 (m, 1H), 7.23 (dd, 2H, J = 8.6, 1.8 Hz), 7.00 (d, 1H, J = 8.2 Hz), 5.05 (s, 2H), 2.54 (s, 6H), 2.07 (s, 3H); ^{13}C {^{1}H} NMR (CD_3Cl, 75 MHz): δ 171.0, 151.4, 141.6, 133.9, 132.9, 128.6 (2C), 128.5, 128.4 (2C), 126.7, 117.5, 66.3, 43.2(2C), 21.1, the signals of the quaternary C atoms were not observed; UV (CH_3CN) λ_{max}/nm (ε/dm^3 mol^{-1} cm^{-1}) = 310 (2660); HRMS (LC-Q/TOF) m/z [M + H]$^+$ Calcd for $C_{17}H_{20}NO_2^+$ 270.1489; Found 270.1501.

(4-(Dimethylamino)-[1,1′-biphenyl]-3-yl)methyl acetate (p,m-OAc). The reaction was carried out according to the procedure for the preparation of esters using a solution of **p,m-OH** (75 mg, 0.3 mmol), TEA (55 μL, 0.4 mmol), and AcCl (28 μL, 0.4 mmol) in anhydrous CH_2Cl_2 (2 mL). The crude product was purified by column chromatography on silica gel using *n*-hexane/CH_2Cl_2 (2:1) as the eluent to give pure product **p,m-OAc** (78 mg, 88%) in the form of colorless oil.

p,m-OAc: ^{1}H NMR (CD_3OD, 300 MHz): δ 7.63 − 7.48 (m, 4H), 7.41 (t, 2H, J = 8.3 Hz), 7.31 (d, 1H, J = 7.4 Hz), 7.25 (d, 1H, J = 8.3 Hz), 5.28 (s, 2H), 2.74 (s, 6H), 2.11 (s, 3H); ^{13}C{1H} NMR (CD_3OD, 75 MHz): δ 172.9, 153.7, 142.0, 137.4, 132.0, 129.8 (2C), 129.3, 128.5, 128.0 (2C), 127.7, 120.9, 63.9, 45.7 (2C), 21.0; UV (CH_3CN) λ_{max}/nm (ε/dm^3 mol^{-1} cm^{-1}) = 281 (13800); HRMS (LC-Q/TOF) m/z [M + H]$^+$ Calcd for $C_{17}H_{20}NO_2^+$ 270.1489; Found 270.1499.

(4′-(Dimethylamino)-[1,1′:3″,1‴-terphenyl]-5′-yl)methyl acetate (p,m-OAc-m-Ph). The reaction was carried out according to the procedure for the preparation of esters, using a solution of **p,m-OH-m-Ph** (150 mg, 0.5 mmol), TEA (164 μL, 1.2 mmol), and AcCl (84 μL, 1.2 mmol) in anhydrous CH_2Cl_2 (5 mL). The crude product was purified by column chromatography on silica gel using *n*-hexane/

Downloaded from pubs.acs.org/joceah/article-pdf/91/17/5947/6205059/acs.joc.6c00228.pdf by RUDJER BOSKOVIC INST user on 05 October 2026

https://doi.org/10.1021/acs.joc.6c00228
J. Org. Chem. 2026, 91, 5947−5968

CH_2Cl_2 (2:1) as the eluent to give pure product **p,m-OAc-m-Ph** (95 mg, 56%) in the form of a colorless oil.

p,m-OAc-m-Ph: ^{1}H NMR ($CDCl_3$, 300 MHz): δ 7.68−7.55 (m, 2H), 7.47−7.26 (m, 10H), 5.30 (s, 2H), 2.56 (s, 6H), 2.15 (s, 3H); ^{13}C {1H} NMR ($CDCl_3$, 75 MHz): δ 171.1, 148.6, 141.9, 140.9, 140.4, 136.7, 134.5, 130.4, 129.2 (2C), 128.7 (2C), 128.1 (2C), 127.3, 127.1, 127.0 (2C), 63.9, 44.2 (2C), 21.2; UV (CH_3CN) λ_{max}/nm (ε/dm^3 mol^{-1} cm^{-1}) = 300 (10273); HRMS (LC-Q/TOF) m/z [M + H]$^+$ Calcd for $C_{23}H_{24}NO_2^+$ 346.1802; Found 314.1814.

(2′-(Dimethylamino)-[1,1′-biphenyl]-3-yl)methyl acetate (o,m′-OAc). The reaction was carried out according to the procedure for the preparation of esters using a solution of **o,m′-OH** (100 mg, 0.4 mmol), TEA (74 μL, 0.5 mmol), and AcCl (38 μL, 0.5 mmol) in anhydrous CH_2Cl_2 (3 mL). The crude product was purified by column chromatography on silica gel using *n*-hexane/CH_2Cl_2 (2:1) as the eluent to give pure product **o,m′-OAc** (70 mg, 59%) in the form of a colorless oil.

o,m′-OAc: ^{1}H NMR ($CDCl_3$, 300 MHz): δ 7.55 (d, 2H, J = 8.6 Hz), 7.39 (t, 1H, J = 7.5 Hz), 7.32− 7.18 (m, 3H), 7.05−6.98 (m, 1H), 5.15 (s, 2H), 2.54 (s, 6H), 2.11 (s, 3H); ^{13}C{1H} NMR ($CDCl_3$, 150 MHz): δ 170.9, 151.2, 142.3, 135.9, 133.5, 131.7, 128.5 (2C), 128.4, 128.3, 126.2, 121.5, 117.6, 66.4, 43.4 (2C), 21.0; UV (CH_3CN) λ_{max}/nm (ε/dm^3 mol^{-1} cm^{-1}) = 270 (4720); HRMS (LC-Q/TOF) m/z [M + H]$^+$ Calcd for $C_{17}H_{20}NO_2^+$ 270.1489; Found 270.1497.

(2′-(Dimethylamino)-[1,1′-biphenyl]-4-yl)methyl acetate (o,p′-OAc). The reaction was carried out according to the procedure for the preparation of esters using a solution of **o,p′-OH** (150 mg, 0.7 mmol), TEA (110 μL, 0.8 mmol), and AcCl (57 μL, 0.8 mmol) in anhydrous CH_2Cl_2 (4 mL). The crude product was purified by column chromatography on silica gel using *n*-hexane/CH_2Cl_2 (2:1) as the eluent to give pure product **o,p′-OAc** (125 mg, 70%) in the form of a white powder.

o,p′-OAc: mp 45−46 °C, ^{1}H NMR ($CDCl_3$, 600 MHz): δ 7.58 (d, 2H, J = 8.1 Hz), 7.37 (d, 2H, J = 8.1 Hz), 7.29−7.26 (m, 1H), 7.20 (dd, 1H, J = 7.5, 1.6 Hz), 7.04 (d, 1H, J = 8.1 Hz), 7.00 (dd, 1H, J = 11.4, 4.1 Hz), 5.14 (s, 2H), 2.54 (s, 6H), 2.13 (s, 3H); ^{13}C {^{1}H} NMR ($CDCl_3$, 75 MHz): δ 171.0, 151.4, 142.2, 134.1, 133.8, 131.8, 129.0 (2C), 128.4 (3C), 128.4, 121.7, 117.8, 66.4, 43.6, 21.2 (2C); UV (CH_3CN) λ_{max}/nm (ε/dm^3 mol^{-1} cm^{-1}) = 274 (5359); HRMS (LC-Q/TOF) m/z [M + H]$^+$ Calcd for $C_{17}H_{20}NO_2^+$ 270.1489; Found 270.1497.

(4′-(Dimethylamino)-[1,1′-biphenyl]-3-yl)methyl acetate (p,m′-OAc). The reaction was carried out according to the procedure for the preparation of esters using a solution of **p,m′-OH** (139 mg, 0.6 mmol), TEA (102 μL, 0.7 mmol) and AcCl (55 μL, 0.7 mmol) in anhydrous CH_2Cl_2 (3 mL). The crude product was purified by column chromatography on silica gel using *n*-hexane/ethyl acetate (2:1) as the eluent to give the pure product **p,m′-OAc** (157 mg, 96%) in the form of a white powder.

p,m′-OAc: mp 61−62 °C, ^{1}H NMR ($CDCl_3$, 300 MHz): δ 7.53−7.48 (m, 4H), 7.39 (t, 1H, J = 8.6 Hz), 7.25 (d, 1H, J = 8.6 Hz), 6.81 (d, 2H, J = 8.6 Hz), 5.15 (s, 2H), 3.00 (s, 6H), 2.12 (s, 3H); ^{13}C{1H} NMR ($CDCl_3$, 150 MHz): δ 171.0, 150.1, 141.3, 133.5, 128.9 (2C), 128.6, 127.7 (2C), 126.4 (2C), 112.7 (2C), 66.3, 40.6 (2C), 21.1; UV (CH_3CN) λ_{max}/nm (ε/dm^3 mol^{-1} cm^{-1}) = 270 (6640); HRMS (LC-Q/TOF) m/z [M + H]$^+$ Calcd for $C_{17}H_{20}NO_2^+$ 270.1489; Found 270.1496.

(4′-(Dimethylamino)-[1,1′-biphenyl]-4-yl)methyl acetate (p,p′-OAc). The reaction was carried out according to the procedure for the preparation of esters, using a solution of **p,p′-OH** (100 mg, 0.4 mmol), TEA (74 μL, 0.5 mmol), and AcCl (38 μL, 0.5 mmol) in anhydrous CH_2Cl_2 (3 mL). The crude product was purified by column chromatography on silica gel using *n*-hexane/CH_2Cl_2 (2:1) as the eluent to give pure product **p,p′-OAc** (60 mg, 51%) in the form of a colorless oil.

p,p′-OAc: ^{1}H NMR ($CDCl_3$, 300 MHz): δ 7.56−7.48 (m, 4H,), 7.38 (d, 2H, J = 8.6 Hz), 6.80 (d, 2H, J = 8.6 Hz), 5.12 (s, 2H), 3.00 (s, 6H), 2.11 (s, 3H); ^{13}C{1H} NMR ($CDCl_3$, 150 MHz): δ 171.0, 150.1, 141.3, 133.5, 128.9 (2C), 128.6, 127.7 (2C), 126.4 (2C), 112.7 (2C), 66.3, 40.6 (2C), 21.1; UV (CH_3CN) λ_{max}/nm (ε/dm^3 mol^{-1} cm^{-1}) = 270 (6700); HRMS (LC-Q/TOF) m/z [M + H]$^+$ Calcd for $C_{17}H_{20}NO_2^+$ 270.1489; Found 270.1491.

Preparation of 6-(Dimethylamino)-[1,1′-biphenyl]-3-carbaldehyde (2). $POCl_3$ (1.03 mL, 11.0 mmol) was added dropwise to the solution of compound **1** (1.8 g, 9.1 mmol) in DMF (6.1 mL) at 0 °C. The mixture was stirred at room temperature under an atmosphere of nitrogen overnight. The reaction mixture was cooled in an ice bath, basified with 10% solution of NaOH (10 mL), and diluted with water (10 mL). The mixture was extracted with ethyl acetate (3 × 30 mL), and the combined organic layers were dried over anhydrous $MgSO_4$ and filtered. The solvent was removed on a rotary evaporator, and the product was separated from the starting material on a column of silica gel using *n*-hexane/ethyl acetate (2:1) as the eluent to obtain 0.75 g (50%) of a yellow-brown oily product **2**. The starting material was regenerated (450 mg), and the synthesis was repeated, yielding 1.50 g of product **2** (27%).

2: ^{1}H NMR (CD_3OD, 600 MHz): δ 9.84 (s, 1H), 7.75 (dd, 1H, J = 8.5, 2.1 Hz), 7.68 (d, 1H, J = 2.1 Hz), 7.51−7.47 (m, 2H), 7.41 (t, 2H, J = 8.5 Hz), 7.34−7.29 (m, 1H), 7.01 (d, 1H, J = 8.5 Hz), 2.68 (s, 6H); ^{13}C{^{1}H} NMR (CD_3OD, 150 MHz): δ 190.8, 156.0, 141.5, 134.5, 131.5, 130.3, 128.6, 128.6 (2C), 128.3 (2C), 127.0, 116.3, 42.7 (2C); HRMS (LC-Q/TOF) m/z [M + H]$^+$ Calcd for $C_{15}H_{16}NO^+$ 226.1226; Found 226.1236.

General Procedure for Coupling the Acyl Halide with (2′-(Dimethylamino)-[1,1′-biphenyl]-4-yl)methanol or (4′-(Dimethylamino)-[1,1′-biphenyl]-3-yl)methanol (o,p′-OH or p,m′-OH)

Alcohol **o,p′-OH** or **p,m′-OH** (0.9 mmol, 0.9 equiv) was dissolved in dry CH_2Cl_2 (7 mL), cooled to 0 °C in an ice bath, and acyl halide **BzOCl** or **PaOCl** (1 mmol, 1 equiv) was added, followed by the addition of DIPEA (1.8 mmol, 1.8 equiv). The reaction mixture was stirred at rt overnight. The solvent was removed on a rotary evaporator, and the crude residue was purified by column chromatography on silica gel using *n*-hexane/CH_2Cl_2 (3:1) as the eluent.

(2′-(Dimethylamino)-[1,1′-biphenyl]-4-yl)methyl benzoate (o,p′-OBz). The synthesis was carried out according to the general procedure described above using alcohol **o,p′-OH** (251 mg, 1.1 mmol), **BzOCl** (172 mg, 1.2 mmol), and DIPEA (385 μL, 2.2 mmol) in dry CH_2Cl_2 (8 mL). The crude product was purified by column chromatography on silica gel using *n*-hexane/CH_2Cl_2 (3:1) as eluent to afford pure compound **o,p′-OBz** (125 mg, 34%) in the form of a colorless oil.

o,p′-OBz: ^{1}H NMR ($CDCl_3$, 600 MHz): δ 8.12 (dd, 2H, J = 8.2, 1.1 Hz), 7.61 (dd, 2H, J = 8.2, 1.1 Hz), 7.58 (td, 1H, J = 8.6, 1.4 Hz), 7.49−7.44 (m, 4H), 7.28 (td, 1H, J = 7.6, 1.8 Hz), 7.22 (dd, 1H, J = 7.6, 1.8 Hz), 7.05 (d, 1H, J = 7.6 Hz), 7.02 (td, 1H, J = 7.6, 1.8 Hz), 5.42 (s, 2H), 2.55 (s, 6H); ^{13}C {^{1}H} NMR ($CDCl_3$, 75 MHz): δ 166.5, 142.0, 134.2, 133.7, 133.0, 131.7, 130.2, 129.7 (2C), 128.9, 128.4 (2C), 128.3, 128.1 (2C), 121.6, 117.7, 66.6, 43.5 (2C). The signals of the quaternary C atoms were not observed; HRMS (LC-Q/TOF) m/z: [M + H]$^+$ Calcd for $C_{22}H_{22}NO_2^+$ 332.1645, Found 332.1645.

(2′-(Dimethylamino)-[1,1′-biphenyl]-4-yl)methyl palmitate (o,p′-OPa). The synthesis was carried out according to the general procedure described above using alcohol **o,p′-OH** (175 mg, 0.8 mmol), **PaOCl** (235 mg, 0.9 mmol), and DIPEA (270 μL, 1.6 mmol) in anhydrous CH_2Cl_2 (6 mL). The product was purified by column chromatography on silica gel using *n*-hexane/CH_2Cl_2 (3:1) as the eluent to afford pure compound **o,p′-OPa** (214 mg, 60%) in the form of a colorless oil.

o,p′-OPa: ^{1}H NMR ($CDCl_3$, 600 MHz,): δ 7.58 (d, 2H, J = 8.2 Hz), 7.38 (d, 2H, J = 8.2 Hz), 7.27 (td, 1H, J = 7.4, 1.6 Hz), 7.21 (dd, 1H, J = 7.4, 1.6 Hz), 7.04 (d, 1H, J = 7.4, 1.6 Hz), 7.01 (td, 1H, J = 7.4, 1.6 Hz), 5.15 (s, 2H), 2.54 (s, 6H), 2.38 (t, 2H, J = 7.6 Hz), 1.71−1.63 (m, 2H), 1.31−1.24 (m, 24H), 0.89 (t, 3H, J = 7.0 Hz); ^{13}C {^{1}H} NMR ($CDCl_3$,150 MHz): δ 173.8, 151.3, 141.9, 134.2, 133.6, 131.6, 128.8 (2C), 128.2, 128.2 (2C), 121.5, 117.6, 66.0, 43.4

Downloaded from pubs.acs.org/joceah/article-pdf/91/17/5947/6205059/acs.joc.6c00228.pdf by RUDJER BOSKOVIC INST user on 05 October 2026

https://doi.org/10.1021/acs.joc.6c00228
J. Org. Chem. 2026, 91, 5947−5968

(2C), 34.4, 31.9, 29.7, 29.7, 29.7, 29.7, 29.6, 29.6, 29.5, 29.4, 29.3, 29.2, 25.0, 22.7, 14.1; HRMS (LC-Q/TOF) *m/z:* $[M + H]^+$ Calcd for $C_{31}H_{48}NO_2^+$ 466.3676, Found 466.3680.

(4′-(Dimethylamino)-[1,1′-biphenyl]-3-yl)methyl benzoate (p,m′-OBz). The synthesis was carried out according to the general procedure described above, using alcohol **p,m′-OH** (183 mg, 0.8 mmol), **BzOCl** (126 mg, 0.9 mmol), and DIPEA (282 μL, 1.6 mmol) in anhydrous CH_2Cl_2 (6 mL). The product was purified by column chromatography on silica gel using *n*-hexane/CH_2Cl_2 (3:1) as the eluent, affording pure compound **p,m′-OBz** (121 mg, 45%) in the form of colorless oil.

p,m′-OBz: ^{1}H NMR ($CDCl_3$, 300 MHz): δ 8.10 (d, 2H, *J* = 7.3 Hz), 7.63 (s, 1H), 7.60−7.48 (m, 4H), 7.48−7.38 (m, 3H), 7.34 (d, 1H, *J* = 7.5 Hz), 6.82 (d, 2H, *J* = 8.4 Hz), 5.42 (s, 2H), 3.00 (s, 6H); ^{13}C {^{1}H} NMR ($CDCl_3$, 150 MHz): δ 166.5, 150.1, 141.7, 136.4, 133.0, 130.2, 129.8 (2C), 128.9, 128.7, 128.4 (2C), 127.8 (2C), 126.2, 126.2, 125.8, 112.8 (2C), 66.9, 40.6 (2C); HRMS (LC-Q/TOF) *m/z:* $[M + H]^+$ Calcd for $C_{22}H_{22}NO_2^+$ 332.1647, Found 332.1645.

(4′-(Dimethylamino)-[1,1′-biphenyl]-3-yl)methyl palmitate (p,m′-OPa). The synthesis was carried out according to the general procedure described above using alcohol **p,m′-OH** (297 mg, 1.3 mmol), **PaOCl** (397 mg, 1.5 mmol), and DIPEA (456 μL, 2.6 mmol) in anhydrous CH_2Cl_2 (9 mL). The product was purified by column chromatography on silica gel using *n*-hexane/CH_2Cl_2 (3:1) as the eluent to afford pure compound **p,m′-OPa** (466 mg, 77%) in the form of colorless oil.

p,m′-OPa: ^{1}H NMR ($CDCl_3$, 300 MHz): δ 7.58−7.44 (m, 4H), 7.38 (t, 1H, *J* = 7.6 Hz), 7.23 (s, 1H), 6.81 (d, 2H, *J* = 8.2 Hz), 5.16 (s, 2H), 3.00 (s, 6H), 2.36 (t, 2H, *J* = 7.5 Hz), 1.71 − 1.61 (m, 2H), 1.39−1.14 (m, 24H), 0.88 (t, 3H, *J* = 6.6 Hz); ^{13}C {^{1}H} NMR ($CDCl_3$,150 MHz): δ 173.8, 150.1, 141.6, 136.5, 128.9, 128.7, 127.7 (2C), 126.1, 126.1, 125.8, 112.7 (2C), 66.2, 40.6 (2C), 34.4, 31.9, 29.7, 29.7, 29.7, 29.7, 29.6, 29.6, 29.5, 29.4, 29.3, 29.2, 25.0, 22.7, 14.1; HRMS (LC-Q/TOF) *m/z:* $[M + H]^+$ Calcd for $C_{31}H_{48}NO_2^+$ 466.3685, Found 466.3680.

3′-((Benzyloxy)methyl)-*N*,*N*-dimethyl-[1,1′-biphenyl]-4-amine (p,m′-OBn). To a solution of benzyl alcohol (49 mg, 0.5 mmol) in anhydrous DMF (4 mL) was added NaH (50% in mineral oil; 65 mg, 2.7 mmol) at −10 °C (ice bath) under an atmosphere of nitrogen. After 20 min at −10 °C, the reaction mixture was stirred for 30 min at rt. The mixture was then cooled back to 0 °C, and the solution of compound **p,m′-Cl** (110 mg, 0.5 mmol) in anhydrous DMF (0.4 mL) was added. The reaction mixture was stirred overnight at rt, then diluted with water (50 mL) and extracted with diethyl ether (3 × 20 mL). The combined extracts were washed with brine (2 × 15 mL) and H_2O (1 × 20 mL) and dried over anhydrous $MgSO_4$. After filtration, the solvent was removed on a rotary evaporator. The crude product was purified by column chromatography on silica gel using *n*-hexane/CH_2Cl_2 (3:1) the eluent, affording compound **p,m′-OBn** (100 mg, 70%) in the form of a yellow oil.

Caution! NaH is a substance which, in contact with water, emits flammable gases and causes skin corrosion and serious eye damage. Care should be taken when handling the substance. Protective eyewear and gloves should be worn.

p,m′-OBn: ^{1}H NMR ($CDCl_3$, 600 MHz): δ 7.56 (s, 1H), 7.53−7.47 (m, 3H), 7.40−7.34 (m, 5H), 7.31−7.26 (m, 2H), 6.81 (d, 2H, *J* = 8.2 Hz), 4.61 (s, 2H), 4.59 (s, 2H), 3.00 (s, 6H); ^{13}C {^{1}H} NMR ($CDCl_3$, 75 MHz): δ 150.0, 141.4, 138.6, 138.4, 129.1, 128.7, 128.4 (2C), 127.8 (2C), 127.7 (2C), 127.6, 125.7, 125.6, 125.5, 112.8 (2C), 72.3, 72.1, 40.6 (2C); HRMS (LC-Q/TOF) *m/z:* $[M + H]^+$ Calcd for $C_{22}H_{24}NO^+$ 318.1856, Found 318.1852.

General Procedure for Coupling Carboxylic Acids with p,m-Cl

Chloride **p,m-Cl** (0.7 mmol, 1 eq) was dissolved in anhydrous CH_2Cl_2 (4.4 mL), cooled to 0 °C (ice bath), and a carboxylic acid derivative (0.6 mmol, 0.9 equiv) was added, followed by the addition of DIPEA (1.7 mmol, 1.8 equiv). The reaction mixture was stirred at rt overnight. The solvent was removed on a rotary evaporator, and the product was purified by column chromatography on silica gel using a mixture of *n*-hexane/CH_2Cl_2 (3:1) as eluent.

(4-(Dimethylamino)-[1,1′-biphenyl]-3-yl)methyl benzoate (p,m-OBz). The synthesis was carried out according to the general procedure described above, using chloride **p,m-Cl** (167 mg, 0.7 mmol), benzoic acid (75 mg, 0.6 mmol), and DIPEA (213 μL, 1.2 mmol) in anhydrous CH_2Cl_2 (4.4 mL). The product was purified by column chromatography on silica gel using *n*-hexane/diethyl ether (15:1) as the eluent, affording pure compound **p,m-OBz** (143 mg, 70%) in the form of a yellow oil.

p,m-OBz: ^{1}H NMR ($CDCl_3$, 600 MHz): δ 8.10 (dd, 2H, *J* = 8.2, 1.2 Hz), 7.72 (s, 1H), 7.59−7.53 (m, 4H), 7.46−7.40 (m, 4H), 7.32 (ddd, 1H, *J* = 7.6, 2.1, 1.2 Hz), 7.22 (d, 1H, *J* = 7.6 Hz), 5.56 (s, 2H), 2.80 (s, 6H); ^{13}C {^{1}H} NMR ($CDCl_3$, 150 MHz): δ 166.7, 152.5, 140.7, 135.9, 133.0, 130.5, 130.3, 129.7 (2C), 128.7, 128.7 (2C), 128.4 (2C), 127.6, 126.9 (2C), 126.9, 119.6, 63.3, 45.3 (2C); HRMS (LC-Q/TOF) *m/z:* $[M + H]^+$ Calcd for $C_{22}H_{22}NO_2^+$ 332.1648, Found 332.1645.

(4-(Dimethylamino)-[1,1′-biphenyl]-3-yl)methyl palmitate (p,m-OPa). The synthesis was carried out according to the general procedure described above using chloride **p,m-Cl** (167 mg, 0.7 mmol), palmic acid (157 mg, 0.6 mmol), and DIPEA (213 μL, 1.2 mmol) in anhydrous CH_2Cl_2 (4.4 mL). The product was purified by column chromatography on silica gel using *n*-hexane/diethyl ether (15:1) as the eluent, affording pure compound **p,m-OPa** (227 mg, 80%) in the form of a yellow oil.

p,m-OPa: ^{1}H NMR ($CDCl_3$, 600 MHz): δ 7.60 (d, 1H, *J* = 2.3 Hz), 7.56 (dt, 2H, *J* = 7.6, 1.2 Hz), 7.52 (dd, 1H, *J* = 8.3, 2.3 Hz), 7.42 (td, 2H, *J* = 7.6, 1.2 Hz), 7.32 (ddd, 1H, *J* = 8.3, 2.3, 1.1 Hz), 7.18 (d, 1H, *J* = 8.3 Hz), 5.30 (s, 2H), 2.75 (s, 6H), 2.38 (t, 2H, *J* = 7.5 Hz), 1.69−1.62 (m, 2H), 1.32−1.21 (m, 24H), 0.88 (t, 3H, *J* = 7.0 Hz); ^{13}C {^{1}H} NMR ($CDCl_3$, 150 MHz): δ 173.9, 152.3, 140.8, 135.8, 130.6, 128.7 (2C), 128.5, 127.4, 126.9, 126.9 (2C), 119.5, 62.6, 45.2 (2C), 34.5, 31.9, 29.7, 29.7, 29.7, 29.7, 29.7, 29.6, 29.5, 29.4, 29.3, 29.2, 25.1, 22.7, 14.1; HRMS (LC-Q/TOF) *m/z:* $[M + H]^+$ Calcd for $C_{31}H_{48}NO_2^+$ 466.3679, Found 466.3680.

General Procedure for the Irradiation of Photocages Ethers and Esters

In a quartz test tube, a compound ether or ester derivative (3 mg, 0.01 mmol) was dissolved in 10 mL CH_3CN and CH_3CN-H_2O (2:1, v/v) in the presence of 50 mM phosphate buffer at pH 7.0. The solution was purged with a stream of Ar or O_2 for 20 min and then irradiated in a Luzchem reactor with 8 lamps (300 nm, 1 lamp, 8W) placed in the middle of the reactor, separated by 15 cm from the lamps on each side. The course of the reaction was followed by HPLC. The irradiated solution was extracted with CH_2Cl_2 (3 × 30 mL). The organic phase was dried over anhydrous $MgSO_4$ and filtered. The solvent was evaporated on a rotary evaporator, and the photoproducts were isolated and characterized by NMR.

Isolation of Photoproduct *N*-((4′-(Dimethylamino)-[1,1′-biphenyl]-3-yl)methyl)acetamide (p,m′-NHAc). In a quartz Erlenmeyer flask, compound **p,m′-OAc** (74 mg, 0.3 mmol) was dissolved in CH_3CN-H_2O (2:1, v/v) in the presence of 50 mM phosphate buffer at pH 7.0. The solution was purged with a stream of N_2 for 1 h and then irradiated in a Luzchem reactor with 8 lamps (300 nm, 1 lamp, 8 W). The irradiated solution was extracted with CH_2Cl_2 (3 × 30 mL). The organic phase was dried over anhydrous $MgSO_4$ and filtered, and the solvent was evaporated on a rotary evaporator. The irradiated mixture was purified on a column of silica gel using *n*-hexane/EtOAc (4:1) as eluent to afford 18 mg of alcohol **p,m′-OH** (28%) and 5 mg of photoproduct **p,m′-NHAc** (7%).

5NHAc: ^{1}H NMR ($CDCl_3$, 300 MHz): δ 7.53−7.44 (m, 4H), 7.36 (t, 1H, *J* = 7.5 Hz), 7.17 (d, 1H, *J* = 7.5 Hz), 6.80 (d, 2H, *J* = 8.7 Hz), 5.75 (bs, 1H), 4.48 (d, 2H, *J* = 5.6 Hz), 3.00 (s, 6H), 2.03 (s, 3H); ^{13}C {^{1}H} NMR ($CDCl_3$,75 MHz): δ 169.9, 141.5, 138.6, 129.1 (2C), 127.9 (2C), 126.0, 125.8, 125.6 (2C), 113.7 (2C), 44.0 (2C), 41.2, 23.3; HRMS (LC-Q/TOF) *m/z:* $[M + H]^+$ Calcd for $C_{17}H_{21}N_2O^+$ 269.1647, Found 269.1648.

Downloaded from pubs.acs.org/joceah/article-pdf/91/17/5947/6205059/acs.joc.6c00228.pdf by RUDJER BOSKOVIC INST user on 05 October 2026

https://doi.org/10.1021/acs.joc.6c00228
J. Org. Chem. 2026, 91, 5947−5968

Preparation of Photoproduct 5′-(Methoxymethyl)-*N*-methyl-[1,1′:3′,1″-terphenyl]-4′-amine (p,m-NHOMe-m-Ph). A methanol solution of phenylboronic acid (260 mg, 1.1 mmol) and a toluene solution of **4** (300 mg, 1.1 mmol) were mixed. Anhydrous potassium carbonate (591 mg, 4.3 mmol) and *tetrakis*-triphenylphosphine palladium $Pd(PPh_3)_4$ (47 mg, 0.05 mmol) were added to the mixture, and the mixture was heated to reflux temperature for 24 h. The next day, after cooling the mixture, H_2O (50 mL) was added, and the layers were separated. The aqueous layer was extracted with CH_2Cl_2 (3 × 30 mL), and the organic layers were combined and dried over anhydrous $MgSO_4$. After filtration, the solvent was removed on a rotary evaporator, and the crude product was purified by column chromatography on silica gel using *n*-hexane/CH_2Cl_2 (1:1) as the eluent to afford product **A** (217 mg, 74%).

In the next step, the product **A** (217 mg, 0.8 mmol) was suspended in anhydrous DMF (5 mL) with Na_2HPO_4 (224 mg, 1.6 mmol), and after that methyl iodide (75 μL; 1.2 mmol) was added. The reaction mixture was stirred at room temperature overnight under a nitrogen atmosphere. The next day, the reaction mixture was diluted with water (20 mL) and extracted with ethyl acetate (3 × 10 mL). The organic layers were combined, washed with brine (2 × 10 mL) and H_2O (1 × 10 mL), then dried over anhydrous $MgSO_4$. After filtration, the solvent was removed on a rotary evaporator. The monomethylated product **B** was separated from the starting material **A** and dimetylated product **p,m-OH** on a column of silica gel using *n*-hexane/ethyl acetate (1:1) as the eluent to obtain 56 mg (24%) of a yellow-brown oily product **B**.

Product **B** (56 mg, 0.2 mmol) was dissolved in dry CH_2Cl_2 (2 mL), cooled to 0 °C by ice bath, and $SOCl_2$ was added (25 μL, 0.3 mmol). The mixture was stirred at 0 °C for 20 min and then 16 h at room temperature. The solvent was removed on a rotary evaporator and product **C** was used in the next step without purification. To a solution of compound **C** (0.2 mmol) in anhydrous methanol (2 mL), a freshly prepared solution of sodium methoxide was added dropwise. The solution of sodium methoxide was prepared by reacting Na (13 mg, 0.6 mmol) in anhydrous methanol (2 mL). The reaction mixture was stirred at rt overnight. Methanol was removed on a rotary evaporator, and CH_2Cl_2 (5 mL) was added to dissolve the product. The reaction solution was washed with H_2O (10 mL), dried over anhydrous $MgSO_4$ and filtered. The solvent was removed on a rotary evaporator, and the product was purified by column chromatography on silica gel using *n*-hexane/CH_2Cl_2 (4:1) as the eluent to give 3 mg (5%) of product **p,m-NHOMe-m-Ph** as a yellow oil.

p,m-NHOMe-m-Ph: ^{1}H NMR ($CDCl_3$, 300 MHz): δ 7.58 (dd, 2H, J = 8.6, 1.2 Hz), 7.52 (dd, 2H, J = 8.6, 1.2 Hz), 7.47−7.36 (m, 6H), 7.34−7.27 (m, 2H), 4.60 (s, 2H), 3.44 (s, 3H), 2.52 (s, 3H); ^{13}C {^{1}H} NMR ($CDCl_3$, 75 MHz): δ 140.5, 130.3, 129.5, 129.1 (2C), 128.9, 128.7 (2C), 128.6 (2C), 128.2, 127.2, 126.7, 126.6 (2C), 73.4, 58.0, 35.9. The signals of the quaternary C atoms were not observed; HRMS (LC-Q/TOF) *m/z*: $[M + H]^+$ Calcd for $C_{21}H_{22}NO^+$ 304.1704, Found 304.1696.

General Procedure for the Photodeprotection of Caged Alcohol p,m′-OBn. In a pyrex glass test tube, compound **p,m′-OBn** (100 mg, 0.3 mmol) was dissolved in 100 mL CH_3CN-H_2O (2:1, v/v) in the presence of 50 mM phosphate buffer at pH 7.0. The solution was purged with a stream of Ar for 30 min, and irradiated in a Rayonet reactor with 10 lamps (300 nm, 1 lamp 8W) placed in the middle of the reactor, separated by 10 cm from the lamps. During the irradiation (40 h), the solution was cooled by a finger tap-H_2O condenser and purged with a stream of Ar. After the irradiation the solvent was evaporated on a rotary evaporator. According to ^{1}H NMR spectrum compounds **p,m′−OH**, **p,m′-OBn** and benzyl alcohol were determined in the ratio 7:10:13.

General Procedure for the Photodeprotection of Caged Acids p,m-OBn, o,p′-OBn, p,m′-OBn, p,m-OPa, o,p′-OPa, and p,m′-OPa. In a Pyrex glass test tube, compound **p,m-OBn**, **o,p′-OBn**, **p,m′-OBn**, **p,m-OPa**, **o,p′-OPa**, or **p,m′-OPa** was dissolved in CH_3CN-H_2O (2:1, v/v) in the presence of 50 mM phosphate buffer at pH 7.0. The solution was purged with a stream of Ar for 0.5−1 h and irradiated in a Rayonet reactor with 10 lamps (300 nm, 1 lamp, 8 W). The irradiated solution was concentrated on a rotary evaporator, and the resulting mixture was shaken with 0.5 M HCl (50 mL) and diethyl ether (20 mL). The organic phase was separated, and the aqueous phase was extracted with diethyl ether (2 × 20 mL). The combined extracts were dried over anhydrous $MgSO_4$ and filtered. The solvent was removed on a rotary evaporator to afford free carboxylic acid. The aqueous phase was basified with 1 M NaOH and extracted with diethyl ether (3 × 20 mL). The organic phase was dried over anhydrous $MgSO_4$ and filtered. The solvent was removed on a rotary evaporator to afford alcohol **p,m-OH**, **o,p′-OH** or **p,m′-OH**.

Irradiation of p,m-OBz. Compound **p,m-OBz** (71 mg, 0.21 mmol) was dissolved in 700 mL of CH_3CN-H_2O (2:1) and irradiated for 5 h in a Rayonet reactor (10 lamps, 300 nm). After the extraction workup, benzoic acid (19 mg, 74%) and alcohol **p,m-OH** (26 mg, 55%) were isolated.

Irradiation of p,m-OPa. Compound **p,m-OPa** (172 mg, 0.37 mmol) was dissolved in 170 mL of CH_3CN-H_2O (2:1) and irradiated for 6 h in a Rayonet reactor (10 lamps, 300 nm). After the extraction workup, palmitic acid (77 mg, 81%) and alcohol **p,m-OH** (45 mg, 54%) were isolated.

Irradiation of o,p′-OBz. Compound **o,p′-OBz** (107 mg, 0.32 mmol) was dissolved in 100 mL of CH_3CN-H_2O (2:1) and irradiated for 4.5 h in a Rayonet reactor (10 lamps, 300 nm). After the extraction workup, benzoic acid (31 mg, 79%) and alcohol **o,p′-OH** (44 mg, 61%) were isolated.

Irradiation of o,p′-OPa. Compound **o,p′-OPa** (179 mg, 0.38 mmol) was dissolved in 180 mL of CH_3CN-H_2O (2:1) and irradiated for 5 h in a Rayonet reactor (10 lamps, 300 nm). After the extraction workup, palmitic acid (89 mg, 90%) and alcohol **o,p′-OH** (65 mg, 75%) were isolated.

Irradiation of p,m′-OBz. Compound **p,m′-OBz** (111 mg, 0.34 mmol) was dissolved in 100 mL of CH_3CN-H_2O (2:1) and irradiated for 9 h in a Rayonet reactor (10 lamps, 300 nm). After the extraction workup, benzoic acid (33 mg, 79%) and 51 mg of a mixture of photoproducts **p,m′-OH** and **p,m′-NHAc** were separated.

Irradiation of p,m′-OPa. Compound **p,m′-OPa** (466 mg, 1.00 mmol) was dissolved in 450 mL of CH_3CN-H_2O (5:1) and irradiated for 14 h in the Rayonet reactor (10 lamps, 300 nm). After the extraction workup, palmitic acid (215 mg, 84%) and 123 mg of a mixture of photoproducts **p,m′-OH** and **p,m′-NHAc** were separated.

Irradiation of o,p′-OAc and p,m′-OAc in the Presence of TEMPO. In a quartz test tube or an Erlenmeyer flask, compound **o,p′-OAc** (50 mg, 0.19 mmol) or **p,m′-OAc** (10 mg, 0.04 mmol) was dissolved in CH_3CN-H_2O (2:1, v/v; 50 or 10 mL) in the presence of a 50 mM phosphate buffer (pH 7.0). TEMPO (108 mg, 0.69 mmol, or 22 mg, 0.14 mmol, respectively) was then added. The solution was purged with a stream of N_2 for 20 min and subsequently irradiated in a Luzchem photoreactor equipped with eight lamps (300 nm, 8 W each). The progress of the reaction was monitored by HPLC. After 1.5 h of irradiation, the reaction mixture was extracted with CH_2Cl_2 (3 × 10 mL). The combined organic layers were dried over anhydrous $MgSO_4$, filtered, and concentrated under reduced pressure using a rotary evaporator. The resulting photoproducts were characterized by NMR and HPLC/MS.

Preparation of Photoproduct (2′-(Methylamino)-[1,1′-biphenyl]-4-yl)methanol (o,p′-NHMeOh). The first step was carried out according to the general methylation procedure described above. To a suspension of *ortho*-bromoaniline (500 mg, 2.9 mmol) and Na_2HPO_4 (825 mg, 5.8 mmol) in dry DMF (2 mL), methyl iodide (220 μL, 3.5 mmol) was added. After the aqueous workup and extraction, the crude product was purified by column chromatography on silica gel using *n*-hexane/CH_2Cl_2 (19:1) as the eluent to afford the monomethylated product **D** (161 mg, 30%) as a yellow oil.

In the next step, compound **D** (161 mg, 0.9 mmol) was subjected to a Suzuki-Miyaura cross-coupling reaction according to the general procedure described above, using a methanolic solution (3 mL) of 4-formylphenylboronic acid (129 mg, 0.9 mmol), a toluene solution (6 mL) of compound **D**, anhydrous potassium carbonate (239 mg, 1.7 mmol), and tetrakis(triphenylphosphine)palladium, $Pd(PPh_3)_4$ (20

Downloaded from pubs.acs.org/joceah/article-pdf/91/17/5947/6205059/acs.joc.6c00228.pdf by RUDJER BOSKOVIC INST user on 05 October 2026

https://doi.org/10.1021/acs.joc.6c00228
J. Org. Chem. 2026, 91, 5947−5968

mg, 0.02 mmol). The product was purified by column chromatography on silica gel using *n*-hexane/CH_2Cl_2 (4:1) as the eluent to afford product **E** (91 mg, 43%) as a yellow solid.

Finally, product **E** (91 mg, 0.43 mmol) was reduced according to the general reduction procedure using $NaBH_4$ (25 mg, 0.65 mmol) in ethanol (5 mL). The crude product was purified by column chromatography on silica gel using *n*-hexane/CH_2Cl_2 (1:1) as the eluent to afford compound **o,p'-NHMeOH** (33 mg, 36%) as a colorless oil.

o,p'-NHMeOH: ^{1}H NMR ($CDCl_3$, 600 MHz): δ 7.45 (d, 2H, J = 8.2 Hz), 7.42 (d, 2H, J = 8.2 Hz), 7.09 (dd, 1H, J = 7.4, 1.6 Hz), 6.78 (td, 1H, J = 7.4, 1.2 Hz), 6.70 (dd, 1H, J = 7.4, 1.2 Hz), 4.75 (s, 2H), 2.80 (s, 3H); ^{13}C {1H} NMR ($CDCl_3$, 150 MHz): δ 146.3 (s), 139.9 (s), 139.1 (s), 130.1 (d), 129.8 (d, 2C), 129.0 (d), 127.7 (d, 2C), 127.3 (s), 117.0 (d), 110.0 (d), 65.3 (t), 30.9 (q).

Quantum Yields of Hydrolysis

Quantum yield measurements for the photohydrolysis reactions of selected photocages in CH_3CN-H_2O (1:1) were carried out in quartz fluorescence cells irradiated exclusively from the front side. KI/KIO_3 was used as the actinometer (Φ_{254} = 0.74).[51] Freshly prepared solutions of the compounds and the actinometer were adjusted to have an absorbance of 0.4−0.8 at 254 nm and were purged with a stream of N_2 for 20 min. The cells with the solutions of actinometer and compounds were placed on the same distance from the lamp (254 nm). The actinometer was irradiated for 60 s, and the solutions of photocages were irradiated for 30 minutes and 1 h, respectively. The conversions of the samples during irradiation were analyzed by HPLC. The measurements were performed in triplicate. Quantum yields were calculated according to eqs S1−S5 in the SI.

Absorption and Fluorescence Measurements

Absorption spectra were recorded on a PG T80/T80+ spectrophotometer at rt. Fluorescence measurements were performed on an Edinburgh FS5 fluorometer using slits corresponding to a bandpass of 1 nm for both excitation and emission. The samples were dissolved in CH_3CN, or CH_3CN-H_2O (1:1, phosphate buffer, pH 7.0, 50 mM), and the concentrations were adjusted to absorbances of less than 0.1 at the excitation wavelengths of 280, 290, 300, 310, 320, 330, and 340 nm. The fluorescence spectra were corrected with respect to the changes in the Xe-lamp intensity and the transmission of the detection monochromator. Fluorescence quantum yields were determined using quinine sulfate in 0.05 M H_2SO_4 as a reference (Φ_f = 0.546).[51] Each fluorescence measurement was performed by exciting the sample at three different wavelengths, and the average value was calculated (eq S6 in the SI). Prior to the measurements, the solutions were purged with Ar for 20 min. The measurements were performed at rt (25 °C).

Laser Flash Photolysis

The measurements were performed on an LP980 Edinburgh Instruments spectrophotometer. For the excitation, the fourth harmonic of a Q-smart Q450 Quantel YAG laser at 266 nm was used. The energy of the laser pulse was set to < 20 mJ, and the pulse duration was 7 ns. Absorbances at the excitation wavelength were set to 0.3. The static cells were used and were frequently exchanged to ensure no absorption of light by photoproducts. The solutions were purged for 20 min with Ar or O_2 prior to the measurements, which were conducted at 25 °C.

Caution! laser irradiation is damaging to biological tissues. Caution is required when working with the laser, and protective eyewear must be worn at all times.

COMPUTATIONAL METHODS

To compute the ground- and S_1-state minimum structures and harmonic vibrational frequencies of the **OAc**, **OMe**, and **OH** biphenylamines (BA), we used density functional theory (DFT) for the ground states and its time-dependent variant (TD-DFT) in the Tamm-Dancoff approximation[61] for the excited states. For all closed-shell singlet species, we used the spin-restricted formalism, and for the doublet radicals, the spin-unrestricted (TD-)DFT formalism. Regarding the exchange-correlation functional, we opted for the range-separated hybrid CAM-B3LYP[62] because it has repeatedly showed good performance in the TDDFT setting.[63,64] In particular, it normally greatly reduces the errors of underestimating the excitation energies of charge transfer and Rydberg states commonly seen with standard hybrid functionals such as B3LYP or PBE0.[63,65,66] The employed Karlsruhe def2-SVPD basis set[67,68] is equipped with sets of polarization and diffuse functions and is contracted to 4s2p2d on the C, N, and O atoms, and 2s2p on the hydrogens. To evaluate the reliability of this basis set,[69] in several instances, we compared the predictions against the extensive def2-TZVPPD basis set (contracted to 6s3p3d1f on the second-row atoms and 3s3p1d on the hydrogens).[68,69] To correct the (TD-)DFT energies for the dispersion interactions, we adopted the recent D4 scheme devised by Grimme et al.[70−72] All computations made use of the high-quality grid designated by "defgrid3" in Orca, which splits the atomic grids into five distinct regions and employs an efficient adaptive pruning scheme depending on the characteristics of the basis set. The highly efficient resolution of identity (RI) approximation technique[73,74] was used based on the def2/J auxiliary Coulomb-fitting basis set.[75] The computation of the HF exchange term was additionally sped up via the chain-of-spheres (RICOSX) algorithm.[76−79] Throughout, we used the conductor-like polarizable continuum model (CPCM)[80] for a fully implicit description of the water solvent, with the dielectric constant set to 80.15. The present algorithm relies on the Gaussian charge scheme with van der Waals-type cavities.[81] In all geometry optimizations, tighter convergence criteria had to be adopted (10^{-6} au in energy and 3×10^{-5} in the RMS gradient) to fully eliminate the unwanted imaginary frequencies of the lowest vibrational modes. At the TD-CAM-B3LYP-D4/def2-SVPD level, we performed the relaxed surface scans[82] in the S_1 state by gradually extending the H_2C-OR bond (R = H, OMe, and OAc) in steps of ca. 0.1 Å, up to 2.8 or 3.0 Å (14−16 scan points in total). By inspecting the Mulliken, Löwdin, and natural (NBO)[83,84] charges on the separating fragments, the bond dissociation process was characterized as either homolytic (charges close to 0) or heterolytic (charges close to ± 1). To confirm the nature of the bond dissociations, at the final scan points (i.e., at the largest H_2C-OR distances), the fragment charges were rechecked with the long-range corrected LC-BLYP exchange-correlation functional.[85−87] This functional was shown to give correct (zero) final charges in the difficult cases of alkali halide dissociation, whereas CAM-B3LYP still predicted some residual charge on the separated atoms.[88] All the computations were performed with the Orca 6.0.1 quantum chemistry program.[89−93]

ASSOCIATED CONTENT

Data Availability Statement

The data underlying this study are openly available via the following link: https://mojoblak.irb.hr/s/smCmiaMfNHiBf23

Supporting Information

The Supporting Information is available free of charge at https://pubs.acs.org/doi/10.1021/acs.joc.6c00228.

Experimental procedures for the synthesis of molecules and photochemical experiments, photophysical data, UV−vis and fluorescence spectra, laser flash photolysis data, computational data, coordinates of the optimized

Downloaded from pubs.acs.org/joceah/article-pdf/91/17/5947/6205059/acs.joc.6c00228.pdf by RUDJER BOSKOVIC INST user on 05 October 2026

https://doi.org/10.1021/acs.joc.6c00228
J. Org. Chem. 2026, 91, 5947−5968

structures, and copies of ^{1}H and ^{13}C NMR spectra (PDF)

AUTHOR INFORMATION

Corresponding Authors

Ivan Ljubić − *Department of Physical Chemistry, Ruđer Bošković Institute, Zagreb 10000, Croatia;* orcid.org/0000-0002-3395-7293; Email: iljubic@irb.hr

Nikola Basarić − *Department of Organic Chemistry and Biochemistry, Ruđer Bošković Institute, Zagreb 10000, Croatia;* orcid.org/0000-0001-9412-9734; Email: nbasaric@irb.hr

Authors

Vilma Lovrinčević − *Department of Organic Chemistry, University of Zagreb Faculty of Chemical Engineering and Technology, Zagreb 10000, Croatia*

Igor Sviben − *Department of Organic Chemistry and Biochemistry, Ruđer Bošković Institute, Zagreb 10000, Croatia*

Mélyne Baudin-Marie − *Department of Organic Chemistry and Biochemistry, Ruđer Bošković Institute, Zagreb 10000, Croatia;* Present Address: Chimie et Interdisciplinarité, Synthèse, Analyze, Modélisation (CEISAM), Nantes Université, CNRS, CEISAM UMR 6230, F-44000

Lidija Uzelac − *Division of Molecular Medicine, Ruđer Bošković Institute, Zagreb 10000, Croatia;* orcid.org/0000-0002-3076-7064

Marijeta Kralj − *Division of Molecular Medicine, Ruđer Bošković Institute, Zagreb 10000, Croatia*

Irena Škorić − *Department of Organic Chemistry, University of Zagreb Faculty of Chemical Engineering and Technology, Zagreb 10000, Croatia;* orcid.org/0000-0002-1563-7261

Dragana Vuk − *Department of Organic Chemistry, University of Zagreb Faculty of Chemical Engineering and Technology, Zagreb 10000, Croatia*

Complete contact information is available at: https://pubs.acs.org/10.1021/acs.joc.6c00228

Author Contributions

#All authors have given approval to the final version of the manuscript.

Notes

The authors declare no competing financial interest.

ACKNOWLEDGMENTS

This research was funded by the Croatian Science Foundation (HRZZ grants no. IP-2022-10-4658 to I.L. and HRZZ-IP-2019-04-8008 and HRZZ-IP-2024-05-8565 to N.B.).

REFERENCES

(1) Ellis-Davies, G. C. R. Reverse Engineering Caged Compounds: Design Principles for their Application in Biology. *Angew. Chem., Int. Ed.* **2023**, *62* (9), No. e202206083.

(2) Bochet, C. G. Photolabile protecting groups and linkers. *J. Chem. Soc., Perkin Trans. 1* **2002**, 125−142.

(3) Pelliccioli, A. P.; Wirz, J. Photoremovable protecting groups: Reaction mechanisms and applications. *Photochem. Photobiol. Sci.* **2002**, *1*, 441−458.

(4) Bochet, C. G. Photochemical release of various functional groups. *Pure Appl. Chem.* **2006**, *78*, 241−247.

(5) Bochet, C. G.; Blanc, A. Photolabile Protecting Groups in Organic Synthesis. In *Handbook of Synthetic Photochemistry*; Albini, A.; Fagnoni, M., Eds.; Wiley-VCH: Weinheim, 2010, pp. 417−447.

(6) Bochet, C. G.; Blanc, A. Photolabile Protecting Groups in Organic Synthesis. In *CRC Handbook of Organic Photochemistry and Photobiology*; Griesbeck, A. G.; Oelgemöller, M.; Ghetti, F., Eds.; CRC Press: Boca Raton, 2012, pp. 73−93.

(7) Wang, P. Photolabile Protecting Groups: Structure and Reactivity. *Asian J. Org. Chem.* **2013**, *2*, 452−464.

(8) Klan, P.; Šolomek, T.; Bochet, C. G.; Blanc, A.; Givens, R.; Rubina, M.; Popik, V.; Kostikov, A.; Wirz, J. Photoremovable Protecting Groups in Chemistry and Biology: Reaction Mechanisms and Efficacy. *Chem. Rev.* **2013**, *113*, 119−191.

(9) Šolomek, T.; Wirz, J.; Klán, P. Searching for Improved Photoreleasing Abilities of Organic Molecules. *Acc. Chem. Res.* **2015**, *48*, 3064−3072.

(10) Peterson, J. A.; Yuan, D.; Winter, A. H. Multiwavelength Control of Mixtures Using Visible Light-Absorbing Photocages. *J. Org. Chem.* **2021**, *86*, 9781−9787.

(11) Shrestha, P.; Mukhopadhyay, A.; Dissanayake, K. C.; Winter, A. H. Efficiency of Functional Group Caging with Second-Generation Green- and Red-Light-Labile BODIPY Photoremovable Protecting Groups. *J. Org. Chem.* **2022**, *87*, 14334−14341.

(12) Weinstain, R.; Slanina, T.; Kand, D.; Klán, P. Visible-to-NIR-Light Activated Release: From Small Molecules to Nanomaterials. *Chem. Rev.* **2020**, *120*, 13135−13272.

(13) Corrie, J. E. T.; Barth, A.; Munasinghe, V. R. N.; Trentham, D. R.; Hutter, M. C. Photolytic Cleavage of 1-(2-Nitrophenyl)ethyl Ethers Involves Two Parallel Pathways and Product Release Is Rate-Limited by Decomposition of a Common Hemiacetal Intermediate. *J. Am. Chem. Soc.* **2003**, *125*, 8546−8554.

(14) Il'ichev, Y. V.; Schwörer, M. A.; Wirz, J. Photochemical reaction mechanisms of 2-nitrobenzyl compounds: Methyl ethers and caged ATP. *J. Am. Chem. Soc.* **2004**, *126*, 4581−4596.

(15) Givens, R. S.; Matuszewski, B. Photochemistry of phosphate esters: An efficient method for the generation of electrophiles. *J. Am. Chem. Soc.* **1984**, *106*, 6860−6861.

(16) Givens, R. S.; Rubina, M.; Wirz, J. Applications of *p*-hydroxyphenacyl (pHP) and coumarin-4-ylmethyl photoremovable protecting groups. *Photochem. Photobiol. Sci.* **2012**, *11*, 472−488.

(17) Takano, M.; Abe, M. Photoreaction of 4-(Bromomethyl)-7-(diethylamino)coumarin: Generation of a Radical and Cation Triplet Diradical during the C-Br Bond Cleavage. *Org. Lett.* **2022**, *24*, 2804−2808.

(18) Givens, R. S.; Jung, A.; Park, C.-H.; Weber, J.; Bartlett, W. New Photoactivated Protecting Groups. 7. *p*-Hydroxyphenacyl: A Phototrigger for Excitatory Amino Acids and Peptides. *J. Am. Chem. Soc.* **1997**, *119*, 8369−8370.

(19) Zhang, K.; Corrie, J. E. T.; Munasinghe, V. N. R.; Wan, P. Mechanism of Photosolvolytic Rearrangement of *p*-Hydroxyphenacyl Esters: Evidence for Excited-State Intramolecular Proton Transfer as the Primary Photochemical Step. *J. Am. Chem. Soc.* **1999**, *121*, 5625−5632.

(20) Conrad, P. G. I. I.; Givens, R. S.; Hellrung, B.; Rajesh, C. S.; Ramseier, M.; Wirz, J. *p*-Hydroxyphenacyl Phototriggers: The Reactive Excited State of Phosphate Photorelease. *J. Am. Chem. Soc.* **2000**, *122*, 9346−9347.

(21) Givens, R. S.; Heger, D.; Hellrung, B.; Kamdzhilov, Y.; Mac, M.; Conrad, P. G. I. I.; Cope, E.; Lee, J. I.; Mata-Segreda, J. F.; Schowen, R. L.; Wirz, J. The Photo-Favorskii Reaction of p-Hydroxyphenacyl Compounds Is Initiated by Water-Assisted, Adiabatic Extrusion of a Triplet Biradical. *J. Am. Chem. Soc.* **2008**, *130*, 3307−3309.

(22) Bownik, I.; Šebej, P.; Literák, J.; Heger, D.; Šimek, Z.; Givens, R. S.; Klán, P. 4-Hydroxyphenacyl ammonium salts: A photoremovable protecting group for amines in aqueous solutions. *J. Org. Chem.* **2015**, *80*, 9713−9721.

Downloaded from pubs.acs.org/joceah/article-pdf/91/17/5947/6205059/acs.joc.6c00228.pdf by RUDJER BOSKOVIC INST user on 05 October 2026

(23) Slanina, T.; Šebej, P.; Heckel, A.; Givens, R. S.; Klán, P. Caged Fluoride: Photochemistry and Applications of 4-Hydroxyphenacyl Fluoride. *Org. Lett.* **2015**, *17*, 4814−4817.
(24) Lukeman, M.; Scaiano, J. C. Carbanion-Mediated Photocages: Rapid and Efficient Photorelease with Aqueous Compatibility. *J. Am. Chem. Soc.* **2005**, *127*, 7698−7699.
(25) Blake, J. A.; Lukeman, M.; Scaiano, J. C. *J. Am. Chem. Soc.* **2009**, *131*, 4127−4135.
(26) Literák, J.; Wirz, J.; Klán, J. 2,5-Dimethylphenacyl carbonates: A photoremovable protecting group for alcohols and phenols. *Photochem. Photobiol. Sci.* **2005**, *4*, 43−46.
(27) Tran, C.; Gallavardin, T.; Petit, M.; Slimi, R.; Dhimane, H.; Blanchard-Desce, M.; Acher, F. C.; Ogden, D.; Dalko, P. I. Two-Photon "Caging" Groups: Effect of Position Isomery on the Photorelease Properties of Aminoquinoline-Derived Photolabile Protecting Groups. *Org. Lett.* **2015**, *17*, 402−405.
(28) Asad, N.; Deodato, D.; Lan, X.; Widegren, M. B.; Phillips, D. L.; Du, L.; Dore, T. M. Photochemical Activation of Tertiary Amines for Applications in Studying Cell Physiology. *J. Am. Chem. Soc.* **2017**, *139*, 12591−12600.
(29) Reinfelds, M.; von Cosel, J.; Falahati, K.; Hamerla, C.; Slanina, T.; Burghardt, I.; Heckel, A. A New Photocage Derived from Fluorene. *Chem.- Eur. J.* **2018**, *24*, 13026−13035.
(30) Hermanns, V.; Scheurer, M.; Kersten, N. F.; Abdellaoui, C.; Wachtveitl, J.; Dreuw, A.; Heckel, A. Rethinking Uncaging: A New Antiaromatic Photocage Driven by a Gain of Resonance Energy. *Chem.- Eur. J.* **2021**, *27*, 14121−14127.
(31) Baird, N. C. Quantum organic photochemistry. II. Resonance and aromaticity in the lowest 3.pi.pi.* state of cyclic hydrocarbons. *J. Am. Chem. Soc.* **1972**, *94*, 4941−4948.
(32) Wang, P. Developing photolabile protecting groups based on the excited state *meta* effect. *J. Photochem. Photobiol., A* **2017**, *335*, 300−310.
(33) Zimmerman, H. E. The Meta Effect in Organic Photochemistry: Mechanistic and Exploratory Organic Photochemistry. *J. Am. Chem. Soc.* **1995**, *117*, 8988−8991.
(34) Wang, P.; Lu, W.; Devalankar, D. A.; Ding, Z. Structurally Simple Benzyl-Type Photolabile Protecting Groups for Direct Release of Alcohols and Carboxylic Acids. *Org. Lett.* **2015**, *17*, 2114−2117.
(35) Ding, X.; Wang, P. Photochemical Cleavage of Benzylic C-O Bond Facilitated by an Ortho or Meta Amino Group. *J. Org. Chem.* **2017**, *82*, 7309−7316.
(36) Škalamera, Đ.; Blažek Bregović, V.; Antol, I.; Bohne, C.; Basarić, N. Hydroxymethylaniline Photocages for Carboxylic Acids and Alcohols. *J. Org. Chem.* **2017**, *82*, 12554−12568.
(37) Ding, X.; Wang, P. 1-[3-(Diethylamino)phenyl]ethyl (DEAPE): A Photolabile Protecting Group for Hydroxyl and Carboxyl Groups. *J. Org. Chem.* **2018**, *83*, 10736−10742.
(38) Wang, P.; Devalankar, D. A.; Lu, W. Photochemical Cleavage of Benzylic C−N Bond To Release Amines. *J. Org. Chem.* **2016**, *81*, 6195−6200.
(39) Wang, P.; Lu, W.; Devalankar, D.; Ding, Z. Photochemical Formation and Cleavage of C−N Bond. *Org. Lett.* **2015**, *17*, 170−172.
(40) Bera, M.; Maji, S.; Paul, A.; Ray, S.; Maiti, T. K.; Singh, N. D. P. A water soluble light activated hydrogen sulfide donor induced by an excited state meta effect. *Org. Biomol. Chem.* **2019**, *17* (40), 9059−9064.
(41) Lovrinčević, V.; Vuk, D.; Škorić, I.; Basarić, N. Chromo-Orthogonal Deprotection of Carboxylic Acids by Aminonaphthalene and Aminoaniline Photocages. *J. Org. Chem.* **2022**, *87*, 2489−2500.
(42) Lovrinčević, V.; Guo, Y.; Vuk, D.; Škorić, I.; Ma, J.; Basarić, N. 3-Substituted 2-Aminonaphthalene Photocages for Carboxylic Acids and Alcohols; Decaging Mechanism and Potential Applications in Synthesis. *J. Org. Chem.* **2023**, *88*, 15176−15188.
(43) Lovrinčević, V.; Zheng, D.; Baudin-Marie, M.; Marić, M.; Uzelac, L.; Škorić, I.; Ma, J.; Vuk, D. Aminonaphthalene and aminoquinoline photocages: Meta-effect and photo-release of carboxylic acids and alcohols. *J. Photochem. Photobiol., A* **2024**, *454*, 115715.
(44) Lipson, M.; Deniz, A. A.; Peters, K. S. Picosecond Kinetic Study of the Dynamics for Photoinduced Homolysis and Heterolysis in Diphenylmethyl Chloride. *J. Phys. Chem.* **1996**, *100*, 3580−3586.
(45) Ammer, J.; Sailer, C. F.; Riedle, E.; Mayr, H. Photolytic Generation of Benzhydryl Cations and Radicals from Quaternary Phosphonium Salts: How Highly Reactive Carbocations Survive Their First Nanoseconds. *J. Am. Chem. Soc.* **2012**, *134*, 11481−11494.
(46) Nguyen, H. D.; Abe, M. Crucial Roles of Leaving Group and Open-Shell Cation in Photoreaction of (Coumarin-4-yl)methyl Derivatives. *J. Am. Chem. Soc.* **2024**, *146*, 10993−11001.
(47) Freccero, M.; Fagnoni, M.; Albini, A. Homolytic vs Heterolytic Paths in the Photochemistry of Haloanilines. *J. Am. Chem. Soc.* **2003**, *125*, 13182−13190.
(48) Wang, Q.; Agarawal, V.; Hermes, M. R.; Motta, M.; Rice, J. E.; Jones, G. O.; Gagliardi, L. Distinguishing homolytic vs heterolytic bond dissociation of phenylsulfonium cations with localized active space methods. *J. Chem. Phys.* **2024**, *161* (1), 014106.
(49) Nguyen, L. T. B.; Abe, M. Study on factors affecting quantum yield for the design of improved *ortho*-nitrobenzyl photoremovable protecting groups. *Bull. Chem. Soc. Jpn.* **2024**, *97* (6), uoae067.
(50) Draženović, J.; Laconsay, C. J.; Došlić, N.; Wu, J. I.-C.; Basarić, N. Excited-state antiaromaticity relief drives facile photoprotonation of carbons in aminobiphenyls. *Chem. Sci.* **2024**, *15*, 5225−5237.
(51) Montalti, M.; Credi, A.; Prodi, L.; Gandolfi, M. T. *Handbook of Photochemistry*; CRC Taylor and Francis: Boca Raton, 2006.
(52) Meech, S. R.; O'Connor, D. V.; Phillips, D.; Lee, A. G. Photophysics of 1-aminonaphthalenes. *J. Chem. Soc., Faraday Trans. 2* **1983**, *79*, 1563−1584.
(53) Arends, I. W. C. E.; Mulder, P.; Clark, K. B.; Wayner, D. D. M. Rate Constants for Termination and TEMPO Trapping of Some Resonance Stabilized Hydroaromatic Radicals in the Liquid Phase. *J. Phys. Chem.* **1995**, *99*, 8182−8189.
(54) Hunter, D. H.; Racok, J. S.; Rey, A. W.; Zea Ponce, Y. Oxoiminium Ions for *N*-Demethylation: l-Oxo-2,2,6,6-tetramethylpiperidinium Chloride. *J. Org. Chem.* **1988**, *53*, 1278−1281.
(55) Najmi, A. A.; Bhat, M. F.; Bischoff, R.; Poelarends, G. J.; Permentier, H. P. TEMPO-Mediated Electrochemical N-demethylation of Opiate Alkaloids. *ChemElectroChem* **2021**, *8*, 2590−2596.
(56) McClelland, R. A.; Kanagasabapathy, V. M.; Banait, N. S.; Steenken, S. Reactivities of triarylmethyl and diarylmethyl cations with azide ion investigated by laser flash photolysis. Diffusion-controlled reactions. *J. Am. Chem. Soc.* **1991**, *113*, 1009−1014.
(57) Perrotta, R. R.; Winter, A. H.; Falvey, D. E. Photochemical Heterolysis of 3,5-Bis(dimethylamino)benzyl Alcohols and Esters: Generation of a Benzyl Cation with a Low-Energy Triplet State. *Org. Lett.* **2011**, *13*, 212−215.
(58) Engkvist, O.; Karlström, G.; Widmark, P.-O. On the origin of the gauche effect. A quantum chemical study of 1,2-difluoroethane. *Chem. Phys. Lett.* **1997**, *265*, 19−23.
(59) Ljubić, I.; Sabljić, A. Fluorocarbonyl oxide: CASSCF/CASPT2 study of structure, *cis* effect and unimolecular decomposition paths. *Chem. Phys.* **2005**, *309*, 157−165.
(60) Schulte, A. M.; Alachouzos, G.; Szymanski, W.; Feringa, B. L. The fate of the contact ion pair determines the photochemistry of coumarin-based photocleavable protecting groups. *Chem. Sci.* **2024**, *15*, 2062−2073.
(61) Hirata, S.; Head-Gordon, M. Time-dependent density functional theory within the Tamm−Dancoff approximation. *Chem. Phys. Lett.* **1999**, *314*, 291−299.
(62) Yanai, T.; Tew, D. P.; Handy, N. C. A new hybrid exchange-correlation functional using the Coulomb-attenuating method (CAM-B3LYP. *Chem. Phys. Lett.* **2004**, *393*, 51−57.
(63) Mandić, L.; Ljubić, I.; Džeba, I. Time-resolved spectroscopic and computational study of the initial events in doxazosin photochemistry. *Spectrochim. Acta, Part A* **2024**, *306*, 123595.
(64) Ljubić, I.; Sviben, I.; Brusar, V.; Zlatić, K.; Vdović, S.; Basarić, N. Competing Photocleavage on Boron and at the *meso*-Position in BODIPY Photocages. *J. Org. Chem.* **2025**, *90*, 259−274.

Downloaded from pubs.acs.org/joceah/article-pdf/91/17/5947/6205059/acs.joc.6c00228.pdf by RUDJER BOSKOVIC INST user on 05 October 2026

https://doi.org/10.1021/acs.joc.6c00228
J. Org. Chem. 2026, 91, 5947−5968

(65) Li, S. L.; Truhlar, D. G. Improving Rydberg Excitations within Time-Dependent Density Functional Theory with Generalized Gradient Approximations: The Exchange-Enhancement-for-Large-Gradient Scheme. *J. Chem. Theory Comput.* **2015**, *11*, 3123−3130.
(66) Liang, J.; Feng, X.; Hait, D.; Head-Gordon, M. Revisiting the Performance of Time-Dependent Density Functional Theory for Electronic Excitations: Assessment of 43 Popular and Recently Developed Functionals from Rungs One to Four. *J. Chem. Theory Comput.* **2022**, *18*, 3460−3473.
(67) Weigend, F.; Ahlrichs, R. Balanced basis sets of split valence, triple zeta valence and quadruple zeta valence quality for H to Rn: Design and assessment of accuracy. *Phys. Chem. Chem. Phys.* **2005**, *7*, 3297−3305.
(68) Rappoport, D.; Furche, F. Property-optimized gaussian basis sets for molecular response calculations. *J. Chem. Phys.* **2010**, *133* (13), 134105.
(69) Bursch, M.; Mewes, J.-M.; Hansen, A.; Grimme, S. Best-Practice DFT Protocols for Basic Molecular Computational Chemistry. *Angew. Chem., Int. Ed.* **2022**, *134* (42), No. e202205735.
(70) Caldeweyher, E.; Bannwarth, C.; Grimme, S. Extension of the D3 dispersion coefficient model. *J. Chem. Phys.* **2017**, *147* (3), 034112.
(71) Caldeweyher, E.; Ehlert, S.; Hansen, A.; Neugebauer, H.; Spicher, S.; Bannwarth, C.; Grimme, S. A generally applicable atomic-charge dependent London dispersion correction. *J. Chem. Phys.* **2019**, *150* (15), 154122.
(72) Caldeweyher, E.; Mewes, J.; Ehlert, S.; Grimme, S. Extension and evaluation of the D4 London-dispersion model for periodic systems. *Phys. Chem. Chem. Phys.* **2020**, *22*, 8499−8512.
(73) Neese, F.; Olbrich, G. Efficient use of the resolution of the identity approximation in time-dependent density functional calculations with hybrid density functionals. *Chem. Phys. Lett.* **2002**, *362*, 170−178.
(74) Neese, F. An improvement of the resolution of the identity approximation for the formation of the Coulomb matrix. *J. Comput. Chem.* **2003**, *24*, 1740−1747.
(75) Weigend, F. Accurate Coulomb-fitting basis sets for H to Rn. *Phys. Chem. Chem. Phys.* **2006**, *8*, 1057−1065.
(76) Neese, F.; Wennmohs, F.; Hansen, A.; Becker, U. Efficient, approximate and parallel Hartree-Fock and hybrid DFT calculations. A 'chain-of-spheres' algorithm for the Hartree-Fock exchange. *Chem. Phys.* **2009**, *356*, 98−109.
(77) Helmich-Paris, B.; de Souza, B.; Neese, F.; Izsák, R. An improved chain of spheres for exchange algorithm. *J. Chem. Phys.* **2021**, *155* (10), 104109.
(78) Izsak, R.; Neese, F. An overlap fitted chain of spheres exchange method. *J. Chem. Phys.* **2011**, *135* (14), 144105.
(79) Izsak, R.; Neese, F.; Klopper, W. Robust fitting techniques in the chain of spheres approximation to the Fock exchange: The role of the complementary space. *J. Chem. Phys.* **2013**, *139* (9), 094111.
(80) Barone, V.; Cossi, M. Quantum calculation of molecular energies and energy gradients in solution by a conductor solvent model. *J. Phys. Chem. A* **1998**, *102*, 1995−2001.
(81) Garcia-Ratés, M.; Neese, F. Effect of the solute cavity on the solvation energy and its derivatives within the framework of the gaussian charge scheme. *J. Comput. Chem.* **2020**, *41*, 922−939.
(82) Petrenko, T.; Kossmann, S.; Neese, F. Efficient time-dependent density functional theory approximations for hybrid density functionals: Analytical gradients and parallelization. *J. Chem. Phys.* **2011**, *134* (5), 054116.
(83) Reed, A. E.; Weinstock, R. B.; Weinhold, F. Natural-population analysis. *J. Chem. Phys.* **1985**, *83*, 735−746.
(84) Glendening, E. D.; Landis, C. R.; Weinhold, F. Natural bond orbital methods. *WIREs Comput. Mol. Sci.* **2012**, *2*, 1−42.
(85) Becke, A. D. Density-functional exchange-energy approximation with correct asymptotic-behavior. *Phys. Rev. A* **1988**, *38*, 3098−3100.
(86) Lee, C.; Yang, W.; Parr, R. G. Development of the Colle-Salvetti correlation-energy formula into a functional of the electron density. *Phys. Rev. B* **1988**, *37*, 785−789.
(87) Iikura, H.; Tsuneda, T.; Yanai, T.; Hirao, K. Long-range correction scheme for generalized-gradient-approximation exchange functionals. *J. Chem. Phys.* **2001**, *115*, 3540−3544.
(88) Bao, J. L.; Verma, P.; Truhlar, D. G. How well can density functional theory and pair-density functional theory predict the correct atomic charges for dissociation and accurate dissociation energetics of ionic bonds? *Phys. Chem. Chem. Phys.* **2018**, *20*, 23072−23078.
(89) Neese, F. Software update: The ORCA program system, version 6.0. *WIREs Comput. Mol. Sci.* **2025**, *15* (2), No. e70019.
(90) Neese, F. Software update: The ORCA program system, version 5.0. *WIREs Comput. Mol. Sci.* **2022**, *12* (5), No. e1606.
(91) Neese, F. The ORCA program system. *WIREs Comput. Mol. Sci.* **2012**, *2*, 73−78.
(92) Neese, F.; Wennmohs, F.; Becker, U.; Riplinger, C. The ORCA quantum chemistry program package. *J. Chem. Phys.* **2020**, *152* (22), 224108.
(93) Neese, F. The SHARK Integral Generation and Digestion System. *J. Comput. Chem.* **2022**, *44*, 381−396.

Downloaded from pubs.acs.org/joceah/article-pdf/91/17/5947/6205059/acs.joc.6c00228.pdf by RUDJER BOSKOVIC INST user on 05 October 2026

https://doi.org/10.1021/acs.joc.6c00228
J. Org. Chem. 2026, 91, 5947−5968